Dicarboxylic acids, oxoacids, benzoic acid, α-dicarbonyls, WSOC, OC, and ions in spring aerosols from Okinawa Island in the western North Pacific Rim: Size distributions and formation processes

D. K. Deshmukh[1], K. Kawamura[1]*, M. Lazaar[1,2], B. Kunwar[1], and S. K. R. Boreddy[1]

[1] Institute of Low Temperature Science, Hokkaido University, Sapporo 060-0819, Japan

[2] Ecole National Supérieure de Chimie de Rennes (ENSCR), Rennes 35708, France

*Corresponding author

E-mail address: kawamura@lowtem.hokudai.ac.jp

Abstract

Size-segregated aerosols (9-stages from <0.43 to >11.3 μm in diameter) were collected at Cape Hedo, Okinawa in spring 2008 and analyzed for water-soluble diacids (C_2-C_{12}), ω-oxoacids (ωC_2-ωC_9), pyruvic acid, benzoic acid and α-dicarbonyls (C_2-C_3) as well as water-soluble organic carbon (WSOC), organic carbon (OC) and major ions (Na^+, NH_4^+, K^+, Mg^{2+}, Ca^{2+}, Cl^-, NO_3^-, SO_4^{2-}, and MSA^-). In all the size-segregated aerosols, oxalic acid (C_2) was found as the most abundant species followed by malonic and succinic acids whereas glyoxylic acid (ωC_2) was the dominant oxoacid and glyoxal (Gly) was more abundant than methylglyoxal. Diacids (C_2-C_5), ωC_2 and Gly as well as WSOC and OC peaked at 0.65-1.1 μm in fine mode whereas azelaic (C_9) and 9-oxononanoic (ωC_9) acids peaked at 3.3-4.7 μm in coarse mode. Sulfate and ammonium are enriched in fine mode whereas sodium and chloride are in coarse mode. Strong correlations of C_2-C_5 diacids, ωC_2 and Gly with sulfate were observed in fine mode (r = 0.86-0.99), indicating a commonality in their secondary formation. Their significant correlations with liquid water content in fine mode (r = 0.82-0.95) further suggest an importance of the aqueous-phase production in Okinawa aerosols. They may have also been directly emitted from biomass burning in fine mode as suggested by strong correlations with potassium (r = 0.85-0.96), which is a tracer of biomass burning. The coarse mode peaks of malonic and succinic acids were obtained in the samples with marine air masses, suggesting that they may be associated with the reaction on sea salt particles. Bimodal size distributions of longer-chain diacid (C_9) and oxoacid (ωC_9) with a major peak in the coarse mode suggest their production by photooxidation of biogenic unsaturated fatty acids via heterogeneous reactions on sea salt particles.

Keywords: Water-soluble organic species, ions, size-segregated aerosols, unimodal distribution, bimodal distribution, secondary aerosols.

1 Introduction

Tropospheric aerosol is an important environmental issue because it can dramatically reduce the visibility (Jacobson et al., 2000; Kanakidou et al., 2005), affect the radiative forcing of climate (Seinfeld and Pandis, 1998), and cause a negative impact on human health (Pope and Dockery, 2006). All of these effects strongly depend on the abundances of aerosols and their chemical and physical properties in different sizes. Particles in diameter of 0.1-1.0 μm are very active in scattering and absorbing incoming solar radiation and have a direct impact on climate (Ramanathan et al., 2001; Seinfeld and Pankow, 2003). The knowledge of size distributions of chemical components is thus essential to better understand their potential contributions to climate change and pollution control. Their size distribution also provides evidences for the sources and formation pathways of the atmospheric particles.

The emission sources and multiple secondary formation pathways of organic aerosols are not well understood. Organic compounds account for up to 70% of fine aerosol mass and potentially control the physicochemical properties of aerosol particles (Davidson et al., 2005; Kanakidou et al., 2005). Low-molecular-weight diacids are one of the most abundant organic compound classes in the atmosphere (Kawamura and Ikushima, 1993; Kawamura et al., 1996). They are primarily derived from incomplete combustion of fossil fuel and biomass burning (Kawamura and Kaplan, 1987; Falkovich et al., 2005), and secondarily produced in the atmosphere via photooxidation of unsaturated fatty acids and volatile organic compounds (VOCs) from biogenic and anthropogenic sources (Kawamura and Gagosian, 1987; Kawamura et al., 1996; Sempéré and Kawamura, 2003). The ability of organic aerosols to act as cloud condensation nuclei (CCN) seems to be closely related to their mass-based size distributions (Pradeep Kumar et al., 2003; Ervens et al., 2007).

The increasing atmospheric burden of organic aerosols is associated with natural and anthropogenic emissions in the continental regions. Organic aerosols are eventually transported to the oceanic regions. The rapid industrialization in East Asia is expected to have important influences on global atmospheric chemistry over the next decades (Wang et al., 2013; Tao et al., 2013; Bian et al., 2014). Large amounts of coal burning and biomass burning in East Asia add more anthropogenic aerosols altering the aerosol chemical composition in the remote Pacific atmosphere

(Mochida et al., 2007; Miyazaki et al., 2010; Agarwal et al., 2010; Wang et al., 2011; Engling et al., 2013). Water-soluble diacids and related compounds as well as major ions are previously studied for their size distributions in remote marine aerosols (Kawamura et al., 2007: Mochida et al., 2007; Miyazaki et al., 2010), whereas their size-segregated characteristics have not been studied in Okinawa Island.

We collected size-segregated aerosol samples with 9-size ranges in spring 2008 in Cape Hedo, Okinawa. Cape Hedo is located on the northern edge of Okinawa Island and can serve as a suitable site for the observation of atmospheric transport of East Asian aerosols with insignificant interference from local emission sources (Takami et al., 2007). The samples were analyzed for dicarboxylic acids (C_2-C_{12}) and related compounds such as ω-oxoacids (ωC_2-ωC_9) and pyruvic acid (C_3) as well as α-dicarbonyls (C_2-C_3) to better understand the sources and processing of water-soluble organic compounds at this marine receptor site in the western North Pacific Rim. Size-segregated samples were also analyzed for water-soluble organic carbon (WSOC), organic carbon (OC), and major inorganic ions. The role of liquid water content of aerosol in the size distribution of diacids and related compounds is discussed. The potential factors responsible for their size distributions and the atmospheric implications of the size characteristics are also discussed.

2 Materials and method

2.1 Site description and aerosol collection

The geographical location of Okinawa Island (26.87°N and 128.25°E) and its surroundings in East Asia are shown in Figure 1. Okinawa is located in the outflow region of continental aerosols and on the pathways to the Pacific. Cape Hedo has been used as a supersite of Atmospheric Brown Clouds project to study the atmospheric transport of Chinese aerosols and their chemical transformation during long-range transport from East Asia (Takiguchi et al., 2008; Kunwar and Kawamura, 2014). The sampling site at Cape Hedo is about 60 m a.s.l.

Size-segregated aerosol samples were collected at Cape Hedo Atmospheric and Aerosol Monitoring Station (CHAAMS) in March 18 to April 13, 2008. This period is characterized by the westerly wind in the lower troposphere, which is the principal process responsible for the transport

of both fossil fuel combustion and biomass burning aerosols in East Asia to the western North Pacific. 9-Stage Andersen Middle Volume Impactor (Tokyo Dylec Company, Japan; 100 L min^{-1}) was used for the collection of size-segregated samples. The sampler was equipped with quartz fiber filters (QFF, 80 mm in diameter) that were pre-combusted at 450°C for 6 h in a furnace to eliminate the adsorbed organic compounds. A total of five sets (OKI-1 to OKI-5) of size-segregated aerosol samples were collected. Each sample set consists of nine filters for the sizes of <0.43, 0.43-0.65, 0.65-1.1, 1.1-2.1, 2.1-3.3, 3.3-4.7, 4.7-7.0, 7.0-11.3, and >11.3 μm. The filter was placed in a preheated 50 mL glass vial with a Teflon-lined screw cap and stored in a freezer at the station. The samples were stored in darkness at -20°C prior to analysis in Sapporo. One set of field blank was collected by placing a pre-combusted QFF for 30s without sucking air before installing real QFF into the sampler.

2.2 Analytical procedures

Diacids and related compounds were analyzed using the method reported in Kawamura and Ikushima (1993), and Kawamura (1993). Aliquot of the filters were extracted with organic-free ultrapure water (specific resistivity >18.2 MΩ-cm) under ultrasonication. The extracts were passed through glass column packed with quartz wool to remove insoluble particles and filter debris. The extracts were concentrated using a rotary evaporator under vacuum and derivatized to dibutyl esters and dibutoxy acetals with 14% BF_3 in *n*-butanol at 100°C. Acetonitrile and *n*-hexane were added into the derivatized sample and washed with organic-free pure water. The hexane layer was further concentrated using a rotary evaporator and dried to almost dryness by N_2 blowdown and dissolve in a known volume of *n*-hexane. A 2 μL aliquot of the sample was injected into a capillary GC (Hewlett-Packard HP6890) equipped with an FID detector. Authentic diacid dibutyl esters were used as external standards for the peak identification and quantification. Identifications of diacids and related compounds were confirmed by GC-mass spectrometry. Recoveries of authentic standards spiked to a pre-combusted QFF were 85% for oxalic acid (C_2) and more than 90% for malonic to adipic (C_3-C_6) acids. The detection limits of diacids and related compounds were ca. 0.002 ng m^{-3}. The analytical errors in duplicate analyses are within 10% for major species.

To measure water-soluble organic carbon (WSOC), a punch of 20 mm diameter of each QFF was extracted with organic-free ultrapure water in a 50 mL glass vial with a Teflon-lined screw cap under ultrasonication for 15 min. The water extracts were subsequently passed through a syringe filter (Millex-GV, Millipore; diameter of 0.22 μm). The extract was first acidified with 1.2 M HCl and purged with pure air in order to remove dissolve inorganic carbon and then WSOC was measured using a total organic carbon (TOC) analyzer (Shimadzu TOC-V_{CSH}) (Miyazaki et al., 2011). External calibration was performed using potassium hydrogen phthalate before analysis of WSOC. The sample was measured three times and the average value was used for the calculation of WSOC concentrations. The analytical error in the triplicate analysis was 5% with a detection limit of 0.1 μgC m^{-3}.

Organic and elemental carbon (OC and EC) was determined using a Sunset Lab carbon analyzer following the Interagency Monitoring of Protected Visual Environments (IMPROVE) thermal evolution protocol as described in detail by Wang et al. (2005a). A filter disc of 1.5 cm^2 was placed in a quartz tube inside the thermal desorption chamber of the analyzer and then stepwise heating was applied. Helium (He) gas is applied in the first ramp and is switched to mixture of He/O_2 in the second ramp. The evolved CO_2 during the oxidation at each temperature step was measured with non-dispersive infrared (NDIR) detector system. The detection limits of OC and EC were ca. 0.05 and 0.02 μgC m^{-3}, respectively. The analytical errors in the triplicate analysis of the filter sample were estimated to be 5% for OC and EC. EC was detected only in fine fractions. The concentration of total carbon (TC) was calculated by summing the concentrations of OC and EC in each size fraction.

For the determination of major ions, a punch of 20 mm diameter of each filter was extracted with organic-free ultrapure water under ultrasonication. These extracts were filtered through a disc filter (Millex-GV, Millipore; diameter of 0.22 μm) and injected to ion chromatograph (Compact IC 761; Metrohm, Switzerland) for measuring MSA^-, Cl^-, SO_4^{2-}, NO_3^-, Na^+, NH_4^+, K^+, Ca^{2+}, and Mg^{2+} (Boreddy and Kawamura, 2015). Anions were separated on a SI-90 4E Shodex column (Showa Denko; Tokyo, Japan) using a mixture of 1.8 mM Na_2CO_3 and 1.7 mM $NaHCO_3$ solution at a flow rate of 1.2 mL min^{-1} as an eluent and 40 mM H_2SO_4 for a suppressor. A Metrosep C2-150 Metrohm

column was used for cation analysis using a mixture of 4 mM tartaric acid and 1 mM dipicolinic acid solution as an eluent at a flow rate of 1.0 mL min^{-1}. The injected loop volume was 200 μL. The detection limits for anions and cations were ca. 0.1 ng m^{-3}. The analytical error in duplicate analysis was about 10%.

Field blanks were extracted and analyzed like the real samples. However, blank levels were 0.1-5% of the concentrations of real samples. The reported concentrations of organic and inorganic species were corrected for the field blanks. All the chemicals including authentic standards were purchased from Wako Pure Chemical Co. (Japan), except for 14% BF_3/n-butanol (Sigma-Aldrich, USA).

2.3 Backward air mass trajectories and meteorology

The backward trajectories of air masses were computed for the sampling period using the Hybrid Single-Particle Lagrangian Integrated Trajectory (HYSPLIT) model 4.0 developed by the National Oceanic and Atmospheric Administration (NOAA) Air Resources Laboratory (ARL) (Draxler and Rolph, 2013). The seven-day trajectories at 500 m above the ground level for the samples collected in Okinawa are shown in Figure 2.

Meteorological data including ambient temperature, relative humidity, wind speed and precipitation for each sample period were obtained from Japan Meteorological Agency (http://www/data/jma.go.jp). During our campaign, the temperature, relative humidity and wind speed ranged from 11.9 to 26.6°C (ave. 20.0±2.61°C), 43.0 to 91.0% (ave. 70.0±12.0%), 0.10 to 10.2 m s^{-1} (ave. 3.73±1.99 m s^{-1}), respectively. The precipitation event occurred occasionally during the campaign with the total amounts of 8.5 mm on March 22 for OKI-1, 9.5 mm on March 25 for OKI-2, 38 mm on March 30 for OKI-3, 18 mm on April 03 and April 06 for OKI-4 and 28 mm on April 13 for OKI-5 sample set.

2.4 Estimation of liquid water content (LWC) of aerosol

LWC of aerosol was calculated for the size-segregated samples collected in Okinawa Island using the ISORROPIA II model (Fountoukis and Nenes, 2007). ISORROPIA II is a computationally efficient and rigorous thermodynamic equilibrium model that exhibits robust and rapid convergence

under all aerosol types with high computational speed (Nenes et al., 1998). ISORROPIA II implies the Zdanovskii-Stokes-Robinson equation and treats only the thermodynamics of K^+ -Ca^{2+} -Mg^{2+} -NH_4^+ -Na^+ -SO_4^{2-} -NO_3^- -Cl^- -H_2O aerosol system to estimate the LWC. Therefore, the measured organic species such as diacids and related compounds are not included in ISORROPIA II. The model was run as "reverse problem", in which temperature, relative humidity and aerosol phase concentrations of water-soluble inorganic ions were used as input for the estimation of aerosol LWC.

3 Results and discussion

3.1 Size-segregated aerosol chemical characteristics

We use 2.1 μm as a split diameter between the fine and coarse mode particles. Table 1 presents the concentrations of inorganic and carbonaceous species in the fine and coarse mode aerosols. Figure 3 shows the average concentrations of inorganic ions and organic matter (OM) in size-segregated aerosols. Abundances of OM in the atmosphere are generally estimated by multiplying the measured OC mass concentrations with the conversion factor of 1.6 for urban aerosols and 2.1 for aged aerosols (Turpin and Lim, 2001). CHAAMS is located in the outflow region of East Asian aerosols and local anthropogenic activities are insignificant. Because the aerosols reaching to Okinawa are subjected to undergo the atmospheric oxidation during the long-range transport, the fraction of oxygenated organic species is often high (Takami et al., 2007; Takiguchi et al., 2008; Kunwar and Kawamura, 2014). Therefore, we used the conversion factor of 2.1, instead of 1.6 for calculation of OM.

Okinawa was strongly affected by continental air masses from Siberia and Mongolia as well as North China and Korea (Figure 2). It is difficult to specify the source regions of air masses for each sample set because the sampling duration was 3-5 days. Each sample contains mixed continental and oceanic air masses. The scavenging of aerosols by precipitation that could result in lower concentrations of aerosol particles in Okinawa might be insignificant during the sampling periods. OM was enriched in fine size fractions than the coarse size fractions (Figure 3). The elevated level of OM in fine fractions in Okinawa (Table 1) suggests a substantial contribution of organic aerosols primarily from combustion sources and secondarily from photochemical processes during long-

range atmospheric transport. The OM in fine mode aerosol in Okinawa might be consists of oxygenated organic compounds such as diacids, ω-oxoacids and α-dicarbonyls.

Sulfate is the most abundant anion in fine fractions with a peak in 0.65-1.1 μm size whereas chloride is the dominant anion in coarse fractions with a maximum in >11.3 μm (Figure 3). The cation budget is largely controlled by ammonium in fine fractions whereas sodium is the most abundant cation in coarse fractions. The high abundance of SO_4^{2-} in fine particles suggests a significant contribution of anthropogenic sources including industrial emissions in East Asia via long-range transport of aerosols over the western North Pacific Rim. SO_4^{2-} is an anthropogenic tracer of industrial activities whereas NH_4^+ is the secondary product of NH_3 that is largely derived from the agricultural usage of nitrogen-based fertilizers (Pakkanen et al., 2001) and volatilization from soils and livestock waste in East Asia (Huang et al., 2006). The dominant presences of Na^+ and Cl^- in coarse fractions suggest a substantial contribution from sea salt. Na^+ and Cl^- are emitted from the ocean surface as relatively larger particles. Substantial amount of NO_3^- was detected in coarse mode, suggesting a formation of $Ca(NO_3)_2$ or $NaNO_3$ in coarse fractions through the reactive adsorption of gaseous HNO_3 onto pre-existing alkaline particles.

Diacids and related compounds detected in Okinawa are listed in Table 2 together with their concentrations in the fine and coarse modes. Their molecular distributions in size-segregated aerosols are shown in Figure 4. Oxalic acid (C_2) was found as the most abundant diacid followed by malonic (C_3) and succinic (C_4) acids in all size-segregated aerosols. The predominance of C_2 in size-segregated aerosols suggested that this diacid is produced by the photooxidation of VOCs and other organic precursors in gas and aqueous-phase (Warneck, 2003; Carlton et al., 2006) during long-range transport. The abundant presence of C_3 over C_4 diacid also indicates that this diacid was produced via atmospheric photooxidation of organic precursors during long-range transport to Okinawa (Kawamura and Sakaguchi, 1999; Kunwar and Kawamura, 2014). They can also be emitted from primary sources such as fossil fuel combustion and biomass burning. Fossil fuel combustion and biomass burning also emit numerous VOCs to the atmosphere, which are ultimately oxidized to diacids via gas and aqueous-phase oxidation.

Phthalic (Ph) and adipic (C_6) acids are the next abundant diacids whereas ketomalonic acid (kC_3) is more abundant than C_6 diacid in the size ranges of 0.43-0.65 μm to 0.65-1.1 μm. Ph and C_6 diacids originate from various anthropogenic sources and thus they can be used as anthropogenic tracers. Ph primarily originates from coal burning and vehicle emission whereas photooxidation of aromatic hydrocarbons such as naphthalene (NAP) and o-xylene derived from incomplete combustion of fossil fuel form Ph via secondary processes (Kawamura and Kaplan, 1987). Moreover, the abundant presence of Ph may also be caused by enhanced emission of phthalates from plastics used in heavily populated and industrialized regions in China and the subsequent long-range atmospheric transport to Okinawa. Phthalic acid esters are used as plasticizers in resins and polymers (Simoneit et al., 2005). They can be released into the air by evaporation because they are not chemically bonded to the polymer. Kawamura and Usukura (1993) reported that C_6 diacid is an oxidation product through the reaction of cyclohexene with ozone (O_3). The high abundances of Ph and C_6 diacids in Okinawa suggest the significant influence of anthropogenic sources in East Asia via long-range transport of aerosols over the western North Pacific Rim.

Azelaic acid (C_9) is always more abundant than the adjacent suberic (C_8) and decanedioic (C_{10}) acids in all the size-segregated aerosols. Kawamura and Gagosian (1987) proposed that C_9 is a photooxidation product of biogenic unsaturated fatty acids such as oleic acid ($C_{18:1}$) containing a double bond at C-9 position. Unsaturated fatty acids can be emitted from sea surface microlayers and from local vegetation in Okinawa (Kunwar and Kawamura, 2014). Moreover, air masses in spring are suggested to originate mostly from Russia and Mongolia as well as Korea based on seven-day backward trajectory analyses. Such continental air masses can also bring C_9 via atmospheric processing of biogenic unsaturated fatty acids during long-range transport. The abundant presence of C_9 indicates that atmospheric oxidation of biogenic unsaturated fatty acids also occurs in Okinawa aerosols during long-range transport. ω-Oxocarboxylic acids and α-dicarbonyls were detected in the Okinawa aerosols. Glyoxylic acid (ωC_2) was identified as the most abundant ω-oxoacid whereas glyoxal (Gly) was more abundant than methylglyoxal (MeGly) in all the sizes. ωC_2 and Gly are the oxidation product of several anthropogenic and biogenic VOCs and primary generated by fossil fuel combustion and biomass burning (Zimmermann and Poppe, 1996;

Volkamer et al., 2001), and are further oxidized to C_2 diacid (Myriokefalitakis et al., 2011). The predominance of ωC_2 and Gly indicates their importance as key precursors of C_2 in Okinawa aerosols.

3.2 Inorganic species

The particle size distributions of major ions are shown in Figure 5. Pearson correlation coefficients (r) among the measured ions in different size modes are given in Table 3. Na^+ and Cl^- are mainly derived from the ocean surface as sea salt particles in the marine atmosphere (Kumar et al., 2008; Geng et al., 2009). The size distributions of Na^+ and Cl^- were found to be bimodal with two peaks in coarse mode (Figure 5a and b). Their peaks at 2.1-3.3 or 3.3-4.7 μm and at >11.3 μm suggest that they are of marine origin due to bubble bursting of surface seawater. Andreas (1998) suggested that the sea spray fall into two types that are defined as film and jet bubbles; film bubbles correspond to the size of 0.5-5 μm whereas jet bubbles produce the size of 5-20 μm. Their coarse mode peaks at 2.1-3.3 μm or 3.3-4.7 as well as >11.3 μm in Okinawa aerosols are associated with film and jet bubbles. We found that size distribution of Mg^{2+} is similar to those of Na^+ and Cl^- with a significant positive correlation to coarse mode Na^+ and Cl^- (r = 0.98), suggesting their similar origin and sources.

A significant contribution of Ca^{2+} in coarse mode particles demonstrates its contributions from soil dust (Kerminen et al., 1997a; Tsai and Chen, 2006). A lifting of soil dust in continental sites followed by subsequent long-range atmospheric transport to remote marine site is also proposed as an important source of Ca^{2+} (Wang et al., 2005b). Ca^{2+} showed unimodal distribution with a peak at either 2.1-3.3 or 3.3-4.7 μm (Figure 5c). The coarse mode Ca^{2+} is mostly derived from crustal $CaCO_3$, which heterogeneously reacts with acidic gases (HNO_3 and SO_2) (Kerminen et al., 1997a). This formation mechanism is further supported by a strong correlation of coarse mode Ca^{2+} with NO_3^- (r = 0.98). There is no correlation between Ca^{2+} and Na^+ or Cl^- (-0.12 or -0.27), revealing that sea salt contribution of Ca^{2+} is negligible in Okinawa aerosols. This result suggests that the long-range transport of soil dust is an important contributor of Ca^{2+} in the marine aerosols from the western North Pacific Rim.

There is natural limestone caves formed by elevating coral reefs in Okinawa Island. Although local limestone dust may also be re-suspended to the atmosphere by wind (Shimada et al., 2015), the contribution of local dust to the Ca^{2+} concentration in Okinawa may be small. This interpretation can be supported by the fact that the peak of Ca^{2+} was appeared in lower coarse size range of 2.1-3.3 or 3.3-4.7 μm. It has been suggested that Ca^{2+} is likely associated with the upper coarse size range when the contribution of locally produced soil particles is significant (Bian et al., 2014). The smaller coarse mode Ca^{2+} is likely associated with long-range transported Asian dust to Okinawa. Moreover, concentrations of Ca^{2+} in coarse mode were found to be much higher in OKI-1 (0.51 μg m^{-3}) and OKI-2 (0.60 μg m^{-3}) than that in OKI-5 sample (0.15 μg m^{-3}). Backward trajectories also indicated that the air masses originated from Mongolia and Siberia are transported to Okinawa during the collection of OKI-1 and OKI-2 samples whereas OKI-5 sample has an influence of marine air masses. Such air mass origin again indicates a long-range transport of Asian dust from East Asia to the western North Pacific.

Potassium is enriched in biomass burning aerosols and therefore its abundances in fine particles can serve as a diagnostic tracer of biomass burning (Yamasoe et al., 2000). Moreover, contributions of K^+ from sea salt and dust sources are highly variable in regional case studies with its dominance in coarse mode particles. Fresh biomass burning particles mostly reside in the condensation mode at 0.1-0.5 μm in diameter whereas the fine mode K^+ of biomass burning origin can be subjected to in-cloud processing (Kaufman and Fraser, 1997; Kleeman and Cass, 1999), in which K^+ can act as effective CCN together with abundant water-soluble organic compounds.

A unimodal size distribution of K^+ was observed in most sets of samples (OKI-1 to OKI-4) with a peak at 0.65-1.1 μm in diameter (Figure 5e). Freshly emitted biomass burning aerosol particles usually exist at the size of 0.1-0.5 μm and thus the peak of K^+ at 0.65-1.1 μm shows that the fine mode K^+ in Okinawa was associated with aged aerosols. Fresh biomass burning aerosols emitted in East Asia might have undergone growth to a relatively large size by absorbing water vapor from the atmosphere during long-range atmospheric transport to Okinawa. The peak of K^+ at 0.65-1.1 μm in fine mode is conceivably a result of a combination of K^+ derived from fresh biomass burning with other water-soluble species such as SO_4^{2-} during long-range transport. This interpretation is

supported by the fact that K^+ showed a positive correlation with LWC (r = 0.83) in fine mode. The fine mode nss-K^+ accounted for 95% of the total K^+ in the OKI-2 sample set and 88% of that in the OKI-3 sample set when air masses are coming from Siberia and Mongolia as well as North China. The abundant presence of fine mode nss-K^+ in the OKI-2 and OKI-3 samples further indicates the long-range atmospheric transport of biomass burning aerosols from the Asian continent to the western North Pacific Rim. The coarse mode K^+ was strongly correlated with the coarse mode Cl^- (r = 0.90). This result suggests that the coarse mode K^+ in the sample sets OKI-1 and OKI-5 may be derived from sea salt particles.

NO_x is known to be a precursor of NO_3^-, which can be converted to HNO_3 and then react with NH_3 to form NH_4NO_3. A unimodal size distribution of NO_3^- was observed with a peak at 2.1-3.3 or 3.3-4.7 μm in diameter. It should also be noted that the NO_3^- concentration in the coarse mode is much higher than that in the fine mode (Table 1). This result suggests that either dust or sea salt particle is the source of coarse mode NO_3^- in Okinawa. Coarse mode NO_3^- is the product of heterogeneous reaction of gaseous NO_2 or HNO_3 with alkaline metals such as Na^+ and Ca^{2+} as shown in Reactions 1 and 2 (Kouyoumdjian and Saliba, 2006; Seinfeld and Pandis, 2006).

$HNO_{3(g)} + NaCl_{(aq\ and\ s)} \rightarrow NaNO_{3(aq\ and\ s)} + HCl_{(g)}$ …… R-1

$2HNO_{3(g)} + CaCO_{3(s)} \rightarrow Ca(NO_3)_{2(s)} + H_2O + CO_{2(g)}$ …… R-2

As discussed earlier, the air masses originated from Siberia are transported over Mongolia and North China. Asian dust can be transported from the Asian continent to Okinawa. Therefore, it is possible that the gaseous HNO_3 might already have reacted with $CaCO_3$ (mineral dust particle) to from NO_3^- before arriving to Okinawa through R-2. We found that coarse mode Na^+, which is derived from sea salts, is negatively correlated (r = -0.30) with the coarse mode NO_3^-. Although this correlation is not significant (p = 0.51), the negative correlation may indicate some reactive loss of NO_3^- from sea salt particles in coarse mode in Okinawa. NO_3^- peaked at the same particle size of Ca^{2+}. Therefore, NO_3^- in Okinawa coarse mode aerosols is probably resulted from the pickup of HNO_3 gas by soil dust particles enriched with Ca^{2+} via heterogeneous reaction near the source regions. This process is further supported by a good correlation between NO_3^- and Ca^{2+} (0.98) in the coarse mode.

335 The particle size distributions of SO_4^{2-}, which is the major source of acid deposition (Pakkanen
336 et al., 2001), have been the subject of numerous studies in the past few decades (Huang et al., 2006;
337 Kouyoumdjian and Saliba, 2006). Condensation mode SO_4^{2-} arises from gas-phase oxidation of SO_2
338 followed by gas-to-particle conversion whereas fine mode SO_4^{2-} is formed through aqueous-phase
339 oxidation of SO_2 in aerosols and cloud droplets (Seinfeld and Pandis, 1998). SO_4^{2-} on the coarse
340 mode can be attributed to a combination of sulfate and heterogeneous reactions of SO_2 on soil dust
341 or sea salt particles (Seinfeld and Pandis, 1998; Pakkanen et al., 2001). A unimodal size distribution
342 of SO_4^{2-} was observed with a peak at 0.65-1.1 μm. The occurrence of SO_4^{2-} at the size of 0.65-1.1
343 μm cannot be explained by gas-phase nucleation or condensation of SO_2. It has also been suggested
344 that in-cloud process produce SO_4^{2-} as larger particles by the oxidation of SO_2 in cloud droplets
345 (Gao et al., 2012), which can become fine particles after the dryness of cloud droplets. This result
346 suggests that the peak of SO_4^{2-} at 0.65-1.1 μm in Okinawa is involved with oxidation of SO_2 with
347 OH radical and O_3 in aerosol aqueous-phase.

348 Secondary inorganic aerosols are major contributors to LWC (Ansari and Pandis, 1999;
349 Engelhart et al., 2011). Calculated LWC for each sample from Okinawa and average LWC in size-
350 segregated aerosols are shown in Figure 6. The most remarkable result of the calculation is the
351 different LWC among the particles of different sizes. We clearly found two peaks of LWC in fine
352 and coarse modes. The difference in LWC in size-segregated aerosols is undoubtedly due to the
353 difference in their chemical composition. We observed that the highest LWC was found at the size
354 of 0.65-1.1 μm in the fine mode in Okinawa samples. As shown in Figure 3, SO_4^{2-} and NH_4^+ are the
355 major ions among the measured inorganic species in fine fractions in Okinawa. High correlation of
356 LWC was found with SO_4^{2-} ($r = 0.92$) in fine mode. This result suggests that an enrichment of SO_4^{2-}
357 in fine mode is enhanced the amount of LWC in fine mode of Okinawa aerosols.

358 Size distribution of methanesulfonate (MSA^-) is similar to that of SO_4^{2-} (Figure 5i) in Okinawa.
359 MSA^- showed a strong correlation with SO_4^{2-} ($r = 0.89$) in fine mode, suggesting that MSA^- should
360 have similar origin with SO_4^{2-} in fine mode. Although MSA^- is believed to be produced by gas-to-
361 particle conversion via the oxidation of dimethyl sulfide (DMS) emitted from the ocean (Quinn et
362 al., 1993; Kerminen et al., 1997b), there is some indirect evidence that liquid-phase production

might also be possible (Jefferson et al., 1998). Biomass burning also produces DMS in the atmosphere (Meinardi et al., 2003; Geng and Mu, 2006). MSA^- showed high correlation with K^+ or NH_4^+ (r = 0.92) in fine mode, indicating that the enhanced emission of DMS from biomass burning followed by the subsequent oxidation during long-range transport may have contributed significantly to the fine mode MSA in Okinawa. Moreover, MSA^- can also be produced in fine mode by the oxidation of DMS that is emitted from the marine phytoplankton in the surrounding ocean. It is noteworthy that East Asian aerosols also travelled over the marine regions including the East China Sea, Sea of Japan and Pacific Ocean during long-range atmospheric transport. This size distribution of MSA^- observed over Okinawa is consistent with previous studies from the China Sea by Gao et al. (1996), who suggested that MSA is produced through the oxidation of S-containing species in the marine atmosphere.

NH_4^+ in the Okinawa aerosols shows a unimodal size distribution with a peak at 0.65-1.1 μm (Figure 5h), indicating that NH_4^+ is mainly formed by gas-to-particle conversion via the reaction with H_2SO_4 and HNO_3. Interestingly, the size distribution of NH_4^+ is similar to that of SO_4^{2-} and diacids such as oxalic acid (Figure 5g and 7a). We also found a strong correlation between SO_4^{2-} and NH_4^+ on the fine mode (r = 0.99). Ion balance calculations are commonly used to evaluate the acid-base balance of aerosol particles. Average equivalent ratios of total cations (Na^+, NH_4^+, K^+, Mg^{2+} and Ca^{2+}) to anions (Cl^-, NO_3^- and SO_4^{2-}) in fine fractions varied from 0.75 for the size bin of 0.65-1.1 μm to 0.86 for the size bin of 1.1-2.1 μm, indicating that fine mode aerosols in Okinawa were apparently acidic.

NH_3 is an alkaline gas that neutralizes the acidic particles in the atmosphere. Kerminen et al. (1997a) proposed that particulate NH_4^+ is secondarily formed via heterogeneous reactions of gaseous NH_3 with acidic species (H_2SO_4 and HNO_3). The reaction of NH_3 with H_2SO_4 is favored over its reaction with HNO_3. The average NH_4^+/SO_4^{2-} equivalent ratios in fine mode particles in Okinawa varied from 0.36 for the size bin of 1.1-2.1 μm to 0.81 for the size bin of 0.43-0.65 μm, indicating that NH_3 was not abundant enough to neutralize all SO_2 and hence H_2SO_4 and NH_4SO_4 were present in addition to $(NH_4)_2SO_4$ in fine mode. Interestingly, the average NH_4^+/SO_4^{2-} equivalent ratios in coarse mode particles ranged from 0.01 for the size bin >11.3 μm to 0.09 for the

size bins of 2.1-3.3 and 3.3-4.7 µm, suggesting that coarse mode aerosols in Okinawa were also NH_4^+-poor. This result further indicates that there was not enough NH_3 to neutralize HNO_3, and thus shortfall of NH_3 may be the restrictive factor for the formation of NH_4NO_3 in Okinawa aerosols. Therefore, NO_3^- reacts with coarse particles that contain alkaline species (Ca^{2+}) in Okinawa aerosols.

The size distribution of SO_4^{2-} also depends on the concentration of NH_4^+, richness of NH_3 in the air, and the presence of coarse mode particles. SO_4^{2-} and NH_4^+ often coexist in fine mode because H_2SO_4 condenses on this mode as fine particles that have more surface area (Jacobson, 2002). Although NH_3 was not abundant enough to neutralize all SO_4^{2-}, most of SO_4^{2-} was neutralize by NH_3 in fine mode and exists in the form of NH_4HSO_4 in addition to $(NH_4)_2SO_4$. Hence, SO_4^{2-} is enriched in fine mode rather than being associated with dust particles. An enrichment of NO_3^- in the dust fraction in our study is supported by the laboratory studies of Hanisch and Crowley (2001a) and (2001b), who found a large and irreversible uptake between HNO_3 and various authentic dust samples including samples from Chinese dust region. We found that NH_4^+ showed a good correlation (r = 0.87) with LWC in the fine mode. This result implies that the abundant presence of NH_4^+ in fine mode also enhanced the LWC in fine mode of Okinawa aerosols. It is notable that higher LWC in fine mode can influence the SOA formation via gas to particle conversion of organic precursors via reactive uptake on aerosols.

3.3 Water-soluble organic carbon (WSOC) and organic carbon (OC)

The mass-based size distribution of WSOC is characterized by a major peak at 0.65-1.1 µm in fine mode and by a small peak at 3.3-4.7 µm in coarse mode (Figure 8 and Table 1). Huang et al. (2006) observed that fine mode WSOC was primarily derived from combustion sources and secondarily produced in the atmosphere by the photochemical oxidation of VOCs. It is well recognized that biofuel combustion and biomass burning produce a large amount of WSOC (Mayol-Bracero et al., 2002). The WSOC concentrations showed high correlation with fine mode SO_4^{2-} (r = 0.96). Because production of SO_4^{2-} is strongly linked to photochemical activity, this result suggests an important secondary production of WSOC in fine mode particles during long-range atmospheric transport from East Asia. The WSOC concentrations also showed high correlation with K^+ (r =

419 0.93) and NH_4^+ (0.91) in the fine mode. This result suggests that direct emission from biomass
420 burning or fast oxidation of biomass burning-derived precursors contributes significantly to the
421 formation of fine mode WSOC in Okinawa aerosols during long-range transport.

422 Fine mode WSOC concentrations in OKI-1 to OKI-4 aerosol samples are 3-5 times higher (1.09
423 μg m^{-3} for OKI-4 to 1.61 μg m^{-3} for OKI-2) than that in the sample OKI-5 (0.31 μg m^{-3}). It is also
424 noteworthy that fine mode fraction of WSOC in the samples OKI-1 to OKI-4 contributed 70-75%
425 of total WSOC. We noted that the former 4 sample sets are more influenced by continental air
426 masses than the last set (Figure 2). These results suggested that WSOC is more enriched in the
427 samples with an influence of continental air masses from Siberia and Mongolia as well as North
428 China and Korea. Because WSOC is an important fraction of OC in Okinawa aerosols, high
429 loadings of WSOC in aerosols of continental air mass origin suggest that both fossil fuel
430 combustion and biomass burning in East Asia may have a significant influence on the composition
431 of water-soluble organic aerosols over the western North Pacific Rim.

432 The mass-size distribution pattern of OC is similar to that of WSOC with a major peak in the
433 size range of 0.65-1.1 μm whereas a small peak was appeared in the size range of 3.3-4.7 μm in
434 diameter (Figure 8). Primary emission from fossil fuel combustion and biomass burning and
435 secondary production from photooxidation of VOCs are considered to be the major sources of OC
436 in atmospheric aerosols (Aggarwal and Kawamura, 2009; Jung et al., 2010). Primary emission from
437 biomass burning or photooxidation of biomass burning derived precursors might be a dominant
438 source of fine mode OC in Okinawa aerosols. This interpretation is supported by the fact that OC
439 showed strong correlation (r = 0.95) with K^+ in fine mode. The fine mode OC showed significant
440 positive correlations with SO_4^{2-} (r = 0.93) and NH_4^+ (r = 0.91), suggesting secondary photochemical
441 formation characteristics of OC in fine mode in Okinawa.

442 A significant portion of OC may be oxidized to WSOC during the atmospheric transport from
443 East Asia to the western North Pacific. The mass ratio of WSOC/OC has been proposed as a
444 measure of photochemical processing or aging of organics especially in long-range transported
445 aerosols (Aggarwal and Kawamura, 2009). The WSOC/OC ratios varied from 0.51-0.76 with an
446 average of 0.67±0.09 in the fine mode and 0.43-0.63 with an average of 0.55±0.09 in the coarse

mode. The higher WSOC/OC ratio in fine mode suggests that organics are more significantly subjected to photochemical processing in fine mode aerosols during long-range transport from the Asian continent to Okinawa than coarse mode aerosols.

Source contributions and secondary processes that may convert VOCs to a more soluble form and surface area of fine particles could cause the higher WSOC/OC ratios in fine mode. Biomass burning-derived OC is highly water-soluble and usually resides in fine mode whereas coarse mode OC contains high molecular weight organic compounds emitted by soil resuspension and emissions of pollens and fungal spores, which are less water-soluble (Wang et al., 2011; Mkoma et al., 2013). Biomass burning significantly contributed to fine mode WSOC in Okinawa and thus WSOC is secondarily produced from oxidation of biomass burning-derived VOCs (Kundu et al., 2010). However, the primary emission of fine mode WSOC from biomass burning could not be excluded. Moreover, accumulation of gas-phase precursors of WSOC may occur preferentially in the particle size with the greatest surface area (Kanakidou et al., 2005). It has been proposed that fine particles offer more surface area and thus reaction rate is more on the surface of fine particles than the coarse particles (Kanakidou et al., 2005). The higher WSOC/OC ratio in fine particles than coarse particles has also been observed in long-range transported East Asian aerosols over Northern Japan (Agarwal et al., 2010).

WSOC also contribute to aerosol LWC although their ability to absorb water is significantly less than that of inorganics (Ansari and Pandis, 2000). Speer et al. (2003) and Engelhart et al. (2011) also noted that inorganic aerosols are associated with 62-80% of aerosol LWC. Moreover, organic species are not taken into account in ISORROPIA II for the calculation of LWC. It is noteworthy that WSOC/OC ratio and LWC significantly correlate in the fine mode with $r = 0.87$ whereas the negative correlation was found in the coarse mode ($r = -0.19$), suggesting the possibility of photochemical production of WSOC from OC in aerosol aqueous-phase in fine mode of Okinawa aerosols. There may also be other important sources of fine mode WSOC in Okinawa aerosols such as primary emission from biomass burning and secondary formation via gas-phase photochemical reactions during long-range atmospheric transport (Hagler et al., 2007; Lim et al., 2010). The strong

474 correlation of WSOC with K^+ in fine mode suggests a substantial contribution of biomass burning
475 to fine mode WSOC in Okinawa aerosols.

476 This result may also indicate that shorter-chain organic compounds with polar functional group
477 such as diacids and oxoacids as well as α-dicarbonyls may contribute more to fine mode WSOC via
478 oxidation of various organic precursors in gas and aqueous-phase during long-range transport
479 (Carlton et al., 2007; Miyazaki et al., 2010). Kawamura et al. (2005, 2007) proposed that shorter-
480 chain diacids and related polar compounds are significantly produced via photochemical oxidation
481 of various precursors and thus they are abundantly present in fine particles contributing more to
482 WSOC fraction.

483 **3.4 Dicarboxylic acids**

484 The size distributions of selected diacids and related compounds are shown in Figure 7. C_2 showed
485 a peak at 0.65-1.1 μm in fine mode (Figure 7a). The monomodal distribution suggests that the
486 heterogeneous uptake of C_2 on sea-salt particles did not occur (Kerminen et al., 1999; Mochida et
487 al., 2003a). The shift of smaller diacids (C_2-C_4) from submicron to supermicron mode has been
488 observed in marine aerosols collected from the western North Pacific in spring when a strong
489 outflow of Asian dusts occurred. Mochida et al. (2003a, 2007) reported that a supermicron peak of
490 diacids was emerged by the uptake of gaseous diacids on sea salt particles based on the similarity
491 between sea salt surface area and diacids size distributions or heterogeneous oxidations of organic
492 precursors on the sea salt particles.

493 The condensation mode of C_2 is likely produced photochemically in the gas-phase followed by
494 condensation onto pre-existing particles at 0.1-0.5 μm (Huang et al., 2006). In the atmosphere, the
495 gas-phase oxidation of isoprene, toluene and ethene leads to the formation of semi-volatile gaseous
496 organic precursors such as Gly and MeGly, which are subsequently participated in aqueous-phase
497 photochemical reaction to result in C_2 diacid (Carlton et al. 2006, 2007; Legrand et al. 2007). The
498 fine mode peak of C_2 at the size of 0.65-1.1 μm in Okinawa aerosols suggests a preferential
499 production of C_2 via the oxidation of precursors in the aerosol aqueous-phase during long-range
500 atmospheric transport. We found that size distribution of C_2 diacid is similar to that of SO_4^{2-} (Figure

5g and 7a), suggesting a secondary formation of C_2 possibly in aerosol aqueous-phase. The good correlations of C_2 with SO_4^{2-} (r = 0.92) and NH_4^+ (r = 0.89) in fine mode further supports that C_2 is a secondary photochemical product. The fine mode C_2 can also be produced primarily from fossil fuel combustion and biomass burning in East Asia and long-range transported to Okinawa. C_2 diacid showed a significant positive correlation with fine mode K^+ (r = 0.85), indicating that biomass burning contributed significantly to fine mode C_2 diacid in Okinawa aerosols.

Several sources are known to C_2 in atmospheric aerosols. They include primary sources and secondary formation via photooxidation of anthropogenic and biogenic precursors (Kawamura and Sakaguchi, 1999). C_2 is produced by the photooxidation of C_3 (Kawamura and Ikushima, 1993). C_2 and C_3 are formed by the photooxidation of C_4 whereas C_4 is produced by the photooxidation of glutaric acid (C_5) (Kawamura and Ikushima, 1993). The fine mode predominance of C_2 in Okinawa aerosols was probably associated with an enhanced aqueous oxidation of anthropogenic precursors emitted in East Asia during long-range transport. Lim et al. (2005) and Legrand et al. (2007) reported the formation of diacids in aqueous-phase. Here we investigate the impact of LWC of aerosols on the formation of diacids in Okinawa aerosols. LWC of a particle can influence the production of C_2 via the changes in gas/particle partitioning of gaseous organic precursors and subsequent heterogeneous reaction in aerosol aqueous-phase. We found that the fine mode peak of C_2 is consistent with that of LWC in Okinawa samples (Figure 6b and 7a). A strong positive correlation (r = 0.92) of C_2 with LWC was found in fine mode. This result supports the possibility of aqueous phase production of C_2 via the oxidation of C_2 precursors in fine mode of Okinawa aerosols.

The robust correlations of C_2 with C_3-C_5 diacids (r = 0.89-0.92) indicate that they have similar sources and origin or C_2 diacid might be produced via decay of longer-chain diacids during long-range transport. This result is further supported by the fact that C_3-C_5 diacids were also enriched in the fine mode (Figure 7b-d) and showed good correlations with LWC (r = 0.82-0.89) possibly due to the enhanced secondary production from oxidation of its precursor compounds in aerosol aqueous-phase. C_2 can also be produced by gas-phase oxidation of various VOCs including toluene, ethene and isoprene followed by subsequent oxidation in aerosol aqueous-phase during long-range

atmospheric transport (Legrand et al., 2007; Lim et al., 2005). The gas-phase photooxidation of these VOCs produce Gly and MeGly, which are easily hydrated and partitioned into the aerosol phase with lifetime less than 3 h (Legrand et al., 2007; Kampf et al., 2012). The aqueous-phase oxidation of Gly and MeGly produces ωC_2, which can further oxidize in aqueous-phase to form C_2 diacid (Lim et al., 2005). It is noteworthy that ωC_2 and Gly are also enriched in fine mode in Okinawa aerosols. Their size distributions are discussed in more details in subsequent sections. Fine mode C_2 showed a significant positive correlation with ωC_2 (r = 0.99) and Gly (0.93) whereas weak correlation was found with MeGly (0.62). These results suggest that ωC_2 and Gly are important precursors of C_2 diacid and increased LWC in fine mode is favorable for aqueous phase oxidation of ωC_2 and Gly to result in C_2.

C_3 peaked at 0.65-1.1 μm in diameter (Figure 7b), being similar to C_2 diacid (Figure 7a), except for two sets of samples (OKI-1 and OKI-5) that showed peaks at 2.1-3.3 or 3.3-4.7 μm in the coarse mode. C_4 showed two peaks at the size bins of 0.65-1.1 and 2.1-3.3 μm in OKI-1 and OKI-5 samples (Figure 7c). The coarse mode peaks of this diacid in samples OKI-1 and OKI-5 may be associated with sea salt particles because the samples have an influence of marine air masses during the sampling period. Kawamura and Ikushima (1993) proposed that the ratio of malonic to succinic acid (C_3/C_4) is a tracer to indicate the extent of photochemical processing of longer chain diacids such as C_5 diacid. Because C_4 is oxidized to C_3, an increase in the C_3/C_4 ratio indicates an increased photochemical processing. The averaged C_3/C_4 ratio in sum of all the size fractions was found to be 1.5±0.1 in Okinawa aerosols. This result suggests that the extent of photochemical processing is much greater in Okinawa than Los Angeles (0.35) (Kawamura and Kaplan, 1987) but similar to that of urban Tokyo (1.5) (Kawamura and Ikushima, 1993), whereas it is lower than those of marine aerosols at Chichijima Island in the western North Pacific (2.0) (Mochida et al., 2003b) and the remote Pacific including tropics (3.9) (Kawamura and Sakaguchi, 1999). Figure 9a shows changes in the C_3/C_4 ratios as a function of particle size. The C_3/C_4 ratios exhibit higher values at 1.1-2.1 μm in fine mode and at 2.1-3.3 and 3.3-4.7 μm in coarse mode. This result suggests that C_3 production via C_4 decomposition occurs more efficiently at these size ranges by aqueous-phase processing.

556 It is noteworthy that emission sources can also control the size distributions of organic
557 compounds. A bimodal size distribution of C_9 diacid was observed in Okinawa aerosols with a
558 major peak on coarse mode at 3.3-4.7 μm and minor peak on fine mode at 0.65-1.1 μm (Figure 7f).
559 C_9 is a tracer of biogenic sources. Kawamura and Gagosian (1987) reported that C_9 is derived from
560 the photooxidation of unsaturated fatty acids such as oleic ($C_{18:1}$) and linoleic ($C_{18:2}$) acids that are
561 produced from the sea surface microlayers to the marine atmosphere with sea salt particles. These
562 unsaturated fatty acids, which are coated in sea salt particles, predominantly reside in the coarse
563 size range (Mochida et al., 2007; Aggarwal et al., 2010). The major peak of C_9 on coarse mode is
564 due to the heterogeneous particle-phase oxidation of unsaturated fatty acids on the sea salt surface.
565 We found significant correlation of C_9 with Na^+ (r = 0.85) in coarse mode. This correlation is
566 consistent with the idea that the precursors of C_9 are emitted from the ocean surface together with
567 sea salt particles in coarse mode. Unsaturated fatty acids can also be directly emitted as fine
568 particles from food cooking emission in China and long-range transported to the western North
569 Pacific (Schauer et al., 1996; Wang et al., 2011). The minor peak of C_9 in fine mode can be
570 explained by the oxidation of fine-mode unsaturated fatty acids derived from food cooking or
571 gaseous unsaturated fatty acids.

572 A unimodal size distribution was obtained for Ph with a fine mode peak at 0.65-1.1 μm, except
573 for one sample set (OKI-5) that showed a bimodal distribution with almost equal peaks at 0.65-1.1
574 and 2.1-3.3 μm (Figure 7g). This aromatic diacid is a tracer of anthropogenic sources. Ph is directly
575 emitted from combustion sources and secondarily produced in the atmosphere by the
576 photooxidation of polycyclic aromatic hydrocarbons such as naphthalene (NAP) and o-xylene
577 derived from incomplete combustion of fossil fuel (Kawamura and Kaplan, 1987). NAP is largely
578 exists in gas-phase and has been suggested to be a major precursor of Ph in the atmosphere
579 (Schauer et al., 1996). The major peak of Ph on fine mode might be due to the preferential
580 production of Ph via gas-phase photooxidation of NAP followed by subsequent condensation onto
581 pre-existing fine mode particles during long-range transport. The high levels of NAP were found in
582 gas-phase and aerosols in source regions in East Asia (Liu et al., 2007; Tao et al., 2007), which
583 indicated NAP as a potential precursor of Ph diacid in Okinawa aerosols. The high levels of

precursors (NAP) in the source regions might favor the significant secondary production of Ph during long-range transport in the western North Pacific. Moreover, the enrichment of Ph in fine mode further suggests that preferential origin of this diacid is related to combustion sources either by primary emission and/or secondary production from the precursor compounds, which is consistent with other anthropogenic constituents such as SO_4^{2-}, NH_4^+ and K^+. The comparable coarse mode peak in the OKI-5 sample set suggests an adsorption of gaseous Ph onto coarse particles. Terephthalic acid (tPh), which is a tracer of plastic burning (Kawamura and Pavuluri, 2011), showed a unimodal distribution peaking at the size bin of 0.65-1.1 μm (Figure 7h). tPh is mostly emitted from the burning of plastic wastes such as plastic bags and bottles, and then deposited on pre-existing fine particles.

Ph diacid originates from various anthropogenic sources whereas C_9 diacid is produced by the oxidation of biogenic unsaturated fatty acids (Kawamura and Gagosian, 1987; Kawamura and Ikushima, 1993). Therefore, Ph/C_9 ratio is mostly used as marker to know the source strength of anthropogenic and biogenic sources of diacids. The higher Ph/C_9 ratio shows more influence of anthropogenic sources whereas lower ratio shows more influence of biogenic sources. Figure 9b shows the changes in the ratios of Ph/C_9 as a function of particle sizes. The higher Ph/C_9 ratios were obtained on the fine mode particles than coarse mode particles. The results suggest that fine aerosols are significantly influenced by anthropogenic sources whereas the coarse aerosols are more influenced by biogenic sources. The significant contribution of Ph on the fine mode demonstrates that this aromatic diacid is mainly produced by the photooxidation of aromatic hydrocarbons such as naphthalene emitted from fossil fuel combustion in gas-phase followed by condensation of the product onto pre-existing fine particles during long-range transport in the atmosphere.

It is important to understand whether anthropogenic or biogenic organic precursors are oxidized to increase the atmospheric level of shorter-chain (C_2-C_5) diacids and related compounds (ωC_2 and Gly) in fine mode of Okinawa aerosols. The strong correlation of C_2-C_5 diacids with Ph (r = 0.83-0.90) was found in fine mode. This result suggests that anthropogenic precursors are more important sources of C_2-C_5 diacids than biogenic precursors in fine mode. The weak correlations of C_2-C_5 diacids with C_9 (r = 0.09-0.38) further suggest that biogenic precursors such as unsaturated

612 fatty acids are not a major source of shorter-chain diacids in fine mode. The higher influences of
613 anthropogenic VOCs than biogenic VOCs can also be evidenced by a lack of correlation (r = 0.25-
614 0.36) between C_2-C_5 diacids and MeGly in fine mode. Myriokefalitakis et al. (2011) proposed that
615 about 80% of MeGly is formed in the atmosphere by the oxidation of biogenic VOCs such as
616 isoprene. Strong correlations of ωC_2 and Gly with Ph (r = 0.90 and 0.85) also suggest that
617 anthropogenic precursors are their major sources in fine mode of Okinawa aerosols.

618 **3.5 ω-Oxocarboxylic acids and pyruvic acid**

619 ω-Oxocarboxylic acids (ωC_2-ωC_9) are secondarily produced in the atmosphere and also directly
620 emitted from fossil fuel combustion and biomass burning. They are further oxidized into diacids via
621 the oxidation of aldehyde group of the compounds (Kawamura et al., 1996; Warneck, 2003). The
622 size distribution of glyoxylic acid (ωC_2) shows a unimodal pattern with a peak at 0.65-1.1 μm
623 (Figure 7i). Mochida et al. (2007) reported a strong bimodal pattern of oxoacids with a peak in the
624 coarse aerosol mode off the coast of East Asia. They suggested that the coarse mode was likely due
625 to either uptake of oxoacids or their heterogeneous reactions on sea salt particles. The fine mode
626 maxima of oxoacids indicate that they are secondarily produced in the atmosphere by the
627 photochemical oxidation of gaseous precursors during long-range transport to Okinawa.
628 Interestingly, we found that size distribution of C_2 diacid is similar to that of ωC_2 oxoacid (Figure
629 7a and i). Those similarities suggest that both C_2 and ωC_2 are simultaneously produced via gas and
630 aqueous-phase oxidation of their precursors. The diacids may be produced by the oxidation of
631 corresponding ω-oxoacids in aerosols during long-range transport.

632 The important precursor of ωC_2 in atmospheric aerosols is Gly and MeGly (Lim et al., 2005;
633 Myriokefalitakis et al., 2011). We found that ωC_2 is strongly correlated with Gly (r = 0.92) and
634 moderately correlated with MeGly (0.55) in the fine mode. The former result suggests that Gly is a
635 key precursor of ωC_2 in Okinawa aerosols. The significant positive correlation of ωC_2 with LWC
636 (0.95) in fine mode suggests the formation of ωC_2 via oxidation of Gly in the aerosol aqueous-
637 phase. The strong correlation of fine mode ωC_2 with SO_4^{2-} (0.96) further confirms secondary
638 formation of ωC_2 from the precursors originated from anthropogenic and biogenic sources during

long-range transport to Okinawa. Although the enhanced ωC_2 concentrations in fine mode might be a result of aqueous oxidation, ωC_2 may be rather controlled by biomass burning activity. This is supported by the significant positive correlation of ωC_2 with K^+ ($r = 0.90$) in the fine mode.

A bimodal size distribution was observed for 9-oxononanoic acid (ωC_9) (Figure 7k). We found that the peak at 3.3-4.7 μm in coarse mode is larger than that at 0.65-1.1 μm in fine mode. The size distribution of ωC_9 is similar to that of C_9 diacid. ωC_9 is another counterpart of photooxidation product of biogenic unsaturated fatty acids such as oleic ($C_{18:1}$) acid having a double bond at C-9 position (Kawamura and Gagosian, 1987). Although air masses during the sampling period are mostly originated from Siberia, Mongolia, Korea and North China (Figure 2), where unsaturated fatty acids of higher plant origin are abundantly supplied to this marine receptor site, sea surface microlayers in the surroundings of Okinawa can also emit unsaturated fatty acids abundantly. The positive correlation of ωC_9 with Na^+ ($r = 0.83$) can also be seen in coarse mode. This suggests that the major peak of ωC_9 on the coarse mode may be due to the heterogeneous oxidation of unsaturated fatty acids of marine phytoplankton origin on the surface of sea salt particles. This result further suggests enhanced input of biogenic organic precursors derived from the ocean on the coarse size range in Okinawa aerosols.

Pyruvic acid (Pyr) showed a bimodal size distribution with a major peak on coarse mode at the size of 3.3-4.7 or 7.0-11.3 μm and a minor peak on fine mode at the size of 0.65-1.1 μm. The larger peak of Pyr on coarse mode may suggest that pyruvic acid is possibly produced by the heterogeneous photooxidation of isoprene emitted from the ocean surface probably on sea salt particles. Several studies suggested that Pyr is produced via the aqueous-phase photooxidation of MeGly that is a gas-phase oxidation product of isoprene emitted from the ocean surface (Lim et al., 2005; Carlton et al., 2006).

3.6 α-Dicarbonyls

Gly and MeGly are gas-phase oxidation products of numerous VOCs such as benzene, toluene and xylene (Volkamer et al., 2001) as well as ethylene and isoprene (Zimmermann and Poppe, 1996) and terpenes (Lim et al., 2005). Gly may be associated with pollution sources whereas MeGly may

be involved with biogenic sources. Gly peaked at 0.65-1.1 μm in the fine mode in the Okinawa samples. The fine mode peak of Gly is similar to those of K^+ and SO_4^{2-} (Figure 5e and g), suggesting their similar sources and formation pathways in the aerosols. Although gas-phase oxidation of isoprene has been reported as the largest global source of Gly (Zimmermann and Poppe, 1996), oxidation of anthropogenic aromatic hydrocarbons from fossil fuel combustion and biomass burning is also suggested as alternative source of Gly in the atmosphere (Jung et al., 2010). The peak of Gly at 0.65-1.1 μm may be associated with the combustion sources and the subsequent gas-phase oxidation of the precursors during long-range transport to Okinawa. A good correlation of Gly with K^+ or NH_4^+ (r = 0.86) in fine mode further suggests that biomass burning is a major source of fine mode Gly in Okinawa aerosols.

In contrast, we found a bimodal size distribution of MeGly with two peaks on the fine and coarse modes. Biogenic VOCs such as isoprene emitted from the ocean surface are subjected to oxidation leading to the formation of MeGly in the atmosphere through aqueous-phase chemistry (Carlton et al., 2006; Ervens et al., 2008). The peak of MeGly on coarse mode suggests that MeGly might be produced by the aqueous-phase oxidation of isoprene emitted from the ocean surface on sea salt particles. MeGly could act as a precursor of secondary organic aerosols (SOA) in the atmosphere (Kroll et al., 2005; Liggio et al., 2005). Gly and MeGly are largely present in gaseous phase and only small portion is in ambient aerosols (Kawamura et al., 2013), although hydrated Gly and MeGly likely exist in aerosols. However, aerosol phase α-dicarbonyls are important in terms of heterogeneous oxidation to result in oxalic acid, which is the most abundant organic species in aerosols. The oxidation of α-dicarbonyls in aerosol phase should promote their transfer from gas to particle phase, affecting the gas/aerosol partitioning of Gly and MeGly, which may have a significant effect on the chemical and physical properties of aerosols.

3.7 Benzoic acid

The size distribution of benzoic acid is presented in Figure 7o. Two sample sets (OKI-1 and OKI-2) showed unimodal size distribution of benzoic acid with a peak at 0.65-1.1 or 1.1-2.1 μm in the fine mode. Benzoic acid is directly emitted from the automobile emissions (Kawamura et al., 1985) and

693 secondarily produced by photochemical oxidation of automobile-derived aromatic compounds (Ho
694 et al., 2006). Although benzoic acid is semi-volatile and mainly found in gas-phase (Kawamura et
695 al., 2000; Fraser et al., 1998), it can be observed in particulate phase via gas-to-particle conversion
696 by forming salts such as ammonium benzoate or potassium benzoate. Duan et al. (2008) reported
697 high level of ambient toluene (11 μg m^{-3}) in China during an ozone episode in 2006 and suggested
698 that photooxidation of toluene is one of major sources of benzoic acid in the atmosphere.

699 The major peak of benzoic acid at small size bin of 0.65-1.1 or 1.1-2.1 μm suggest that a
700 significant portion of this compound in the Okinawa aerosols is likely produced by gas-to-particle
701 conversion via the reaction with NH_3 and alkaline metals and the subsequent deposition onto pre-
702 existing fine particles during long-range transport. We observed an additional small peak of benzoic
703 acid at 4.7-7.0 μm on the coarse mode for the sample sets of OKI-3 to OKI-5. Because benzoic acid
704 mainly exists in gas-phase in the atmosphere due to the relatively high volatility (Fraser et al., 1998),
705 the small peak on the coarse mode indicates a potential adsorption of gaseous benzoic acid onto
706 larger particles that may contain alkaline Na, K and Ca, or uptake by sea spray water droplets
707 emitted from sea surface.

708 **4 Summary and conclusions**

709 Nine-stage aerosol particles from <0.43 to >11.3 μm in diameter, collected in spring 2008 at Cape
710 Hedo, Okinawa in the western North Pacific Rim, were analyzed for water-soluble diacids and
711 related compounds as well as major ions. The molecular distributions of diacids were characterized
712 by the predominance of oxalic acid (C_2) followed by malonic (C_3) and succinic (C_4) acids in all
713 stages, suggesting that they are most likely produced by the photooxidation of VOCs and particulate
714 organic precursors in the source region and/or during long-range atmospheric transport. The
715 abundant presence of SO_4^{2-} as well as phthalic and adipic acids in Okinawa suggested the
716 significant contributions of anthropogenic sources including industrial emissions in East Asia via
717 long-range atmospheric transport.

718 SO_4^{2-}, NH_4^+, and diacids up to 5-carbon atoms as well as glyoxylic acid (ωC_2) and glyoxal (Gly)
719 showed good correlations with peaks in fine mode (0.65-1.1 μm). WSOC and OC also peaked on

720 fine mode with an additional minor peak on coarse mode. Similar size distributions and strong
721 correlations of diacids (C_2-C_5), ωC_2 and Gly with SO_4^{2-} in fine mode suggest their secondary
722 formation possibly in the aerosol aqueous-phase. They may have also been directly emitted from
723 biomass burning as suggested by strong correlations with K^+ in fine mode. The strong correlations
724 of fine mode SO_4^{2-} and NH_4^+ with LWC imply that abundant presences of SO_4^{2-} and NH_4^+ in fine
725 mode promote to enhance the LWC in fine mode of Okinawa aerosols, which is favorable for the
726 aqueous oxidation of precursor compounds to result in C_2 (r is 0.91 for LWC and C_2). The robust
727 correlations of C_2 with C_3-C_5 diacids as well as ωC_2 and Gly indicate that they are the key
728 precursors of C_2 diacid in Okinawa aerosols.

729 We observed an enrichment of C_3 and C_4 diacids on coarse mode particles in the aerosols with
730 marine air mass origin, indicating that their formation is associated with the heterogeneous
731 reactions on sea salt particles. Longer-chain diacid (C_9) and ω-oxoacid (ωC_9) showed bimodal size
732 distribution with a major peak on coarse mode, suggesting that they are produced by photooxidation
733 of unsaturated fatty acids mainly derived from phytoplankton via heterogeneous reactions on sea
734 spray particles. We observed that WSOC and OC in fine particles are photochemically more
735 processed in the atmosphere than in coarse particles during long-range transport. This study
736 demonstrates that anthropogenic and biomass burning aerosols emitted from East Asia have
737 significant influence on the molecular compositions of water-soluble organic aerosols in the
738 western North Pacific Rim.

739 **Acknowledgement**

740 We acknowledge the financial support from the Japan Society for the Promotion of Science (JSPS)
741 through Grant-in-Aid Nos. 1920405 and 24221001. We appreciate the financial support of the JSPS
742 fellowship to D. K. Deshmukh. We also acknowledge the support of ENSCR to M. Lazaar for the
743 summer student program in Japan. The authors gratefully appreciate the NOAA Air Resources
744 Laboratory (ARL) for the provision of the HYSPLIT transport and dispersion model
745 (http://www.ready.noaa.gov) for seven-day air mass backward trajectories of sampling site Cape
746 Hedo for each sampling period. We thank E. Tachibana for the analyses of OKI-5 samples and M.

747 Mochida, S. Aggarwal and Y. Kitamori for the helps during the campaign. The authors appreciate
748 the critical and useful comments by anonymous reviewers, which significantly improved the quality
749 of manuscript.
750

751 **References**

752 Ansari, A. S. and Pandis, S. N.: Prediction of multicomponent inorganic atmospheric aerosol
753 behavior, Atmos. Environ., 33, 745-757, 1999.

754 Ansari, A. S. and Pandis, S. N.: Water absorption by secondary organic aerosol and its effect on
755 inorganic aerosol behavior, Environ. Sci. Technol., 34, 71-77, 2000.

756 Agarwal, S., Aggarwal, S. G., Okuzawa, K., and Kawamura, K.: Size distributions of dicarboxylic
757 acids, ketoacids, alpha-dicarbonyls, sugars, WSOC, OC, EC and inorganic ions in
758 atmospheric particles over Northern Japan: implication for long-range transport of Siberian
759 biomass burning and East Asian polluted aerosols, Atmos. Chem. Phys., 10, 5839-5858,
760 2010.

761 Aggarwal, S. G. and Kawamura, K.: Carbonaceous and inorganic composition in long-range
762 transported aerosols over northern Japan: implicationsn for aging of water-soluble organic
763 fraction, Atmos. Environ., 43, 2532-2540, 2009.

764 Andreas, E.L.: A new sea spray generation function for wind speeds up to 32 m s^{-1}, J. Phys.
765 Oceanogr., 28, 2175-2184, 1998.

766 Bian, Q., Huang, X. H. H., and Yu, J. Z.: One-year observations of size distribution characteristics
767 of major aerosol constituents at a costal site in Hong Kong - Part 1: Inorganic ions and
768 oxalate, Atmos. Chem. Phys., 14, 9013-9027, 2014.

769 Boreddy, S. K. R. and Kawamura K.: A 12-year observation of water-soluble inorganic ions in TSP
770 aerosols collected at a remote marine location in the western North Pacific: An outflow region
771 of Asian dust, Atmos. Chem. Phys., 15, 6437-6453, 2015.

772 Carlton, A. G., Turpin, B. J., Altieri, K. E., Seitzinger, S., Reff, A., Lim, H. J., and Ervens, B.:
773 Atmospheric oxalic acid and SOA production from glyoxal: Results of aqueous
774 photooxidation experiments, Atmos. Environ., 41, 7588-7602, 2007.

775 Carlton, A. G., Turpin, B. J., Lim, H. J., Altieri, K. E., and Seitzinger, S.: Link between isoprene
776 and secondary organic aerosol (SOA): Pyruvic acid oxidation yields low volatility organic
777 acids in clouds, Geophys. Res. Lett., 33, L06822, doi:10.1029/2005GL025374, 2006.

778 Davidson, C. I., Phalen, R. F., and Solomon, P. A.: Airborne particulate matter and human health: A
779 review, Aerosol. Sci. Tech., 39, 737-749, 2005.

780 Draxler, R. R. and Rolph, G. D.: HYSPLIT (HYbrid Single-Particle Lagrangian Integrated Trajec-
781 tory) Model, available at: http://www.arl.noaa.gov/HYSPLIT.php (last access: 5 January
782 2015), NOAA Air Resouces Laboratory, College Park, MD.

783 Duan, J. C., Tan, J. H., Yang, L., Wu, S., and Hao, J. M.: Concentration, sources and ozone
784 formation potential of volatile organic compounds (VOCs) during ozone episode in Beijing,
785 Atmos. Res., 88, 25-35, 2008.

786 Engelhart, G. J., Hildebrandt, L., Kostenidou, E., Mihalopoulos, N., Donahue, N. M., and Pandis, S.
787 N.: Water content of aged aerosol, Atmos. Chem. Phys., 11, 911-920, 2011.

788 Engling, G., Lee, J. J., Sie, H. J., Wu, Y. C., and Yet-Pole, I.: Anhydrosugar characteristics in
789 biomass smoke aerosol-case study of environmental influence on particle-size of rice straw
790 burning aerosol, J. Aerosol Sci., 56, 2-14, 2013.

Ervens, B., Carlton, A. G., Turpin, B. J., Altieri, K. E., Kreidenweis, S. M., and Feingold, G.: Secondary organic aerosol yields from cloud-processing of isoprene oxidation products, Geophys. Res. Lett., 35, L02816, doi:10.1029/2007gl031828, 2008.

Ervens, B., Cubison, M., Andrews, E., Feingold, G., Ogren, J. A., Jimenez, J. L., DeCarlo, P., and Nenes, A.: Prediction of cloud condensation nucleus number concentration using measurements of aerosol size distributions and composition and light scattering enhancement due to humidity, J. Geophys. Res., 112, D10S32, doi:10.1029/2006jd007426, 2007.

Ervens, B. and Volkamer, R.: Glyoxal processing by aerosol multiphase chemistry: towards a kinetic modeling framework of secondary organic aerosol formation in aqueous particles, Atmos. Chem. Phys., 10, 8219-8244, 2010.

Falkovich, A. H., Graber, E. R., Schkolnik, G., Rudich, Y., Maenhaut, W., and Artaxo, P.: Low molecular weight organic acids in aerosol particles from Rondonia, Brazil, during the biomass-burning, transition and wet periods, Atmos. Chem. Phys., 5, 781-797, 2005.

Fountoukis, C. and Nenes, A.: ISORROPIA II: a computationally efficient thermodynamic equilibrium model for K^+-Ca^{2+}-Mg^{2+}-NH_4^+-Na^+-SO_4^{2-}-NO_3^--Cl^--H_2O aerosols, Atmos. Chem. Phys., 7, 4639-4659, 2007.

Fraser, M. P., Cass, G. R., and Simoneit, B. R. T.: Gas-phase and particle-phase organic compounds emitted from motor vehicle traffic in a Los Angeles roadway tunnel, Environ. Sci. Technol., 32, 2051-2060, 1998.

Gao, Y., Arimoto, R., Duce, R. A., Chen, L. Q., Zhou, M. Y., and Gu, D. Y.: Atmospheric non-sea-salt sulfate, nitrate and methanesulfonate over the China Sea, J. Geophys. Res., 101, 12601-12611, 1996.

Gao, X., Xue, L., Wang, X., Wang, T., Yuan, T., Gao, R., Zhou, Y., Nie, W., Zhang, Q., and Wang, W.: Aerosol ionic components at Mt. Heng in central southern China: abundances, size distribution, and impacts of long-range transport, Sci. Total Environ., 433, 498-506, 2012.

Geng, H., Park, Y., Hwang, H., Kang, S., and Ro, C. U.: Elevated nitrogen-containing particles observed in Asian dust aerosol samples collected at the marine boundary layer of the Bohai Sea and the Yellow Sea, Atmos. Chem. Phys., 9, 6933-6947, 2009.

Geng, C. and Mu, Y: Carbonyl sulfide and dimethyl sulfide exchange between trees and the atmosphere, Atmos. Environ., 40, 1373-1383, 2006.

Hagler, G. S. W., Bergin, M. H., Smith, E. A., and Dibb, J. E.: A summer time series of particulate carbon in the air and snow at Summit, Greenland, J. Geophys. Res., 112, D21309, doi:10.1029/2007JD008993, 2007.

Hanisch, F. and Crowley, J.N.: Heterogeneous reactivity of gaseous nitric acid on Al_2O_3, $CaCO_3$, and atmospheric dust samples: A Knudsen cell study, J. Phys.Chem. (A), 105, 3096-3106, 2001a.

Hanisch, F. and Crowley, J.N.: The heterogeneous reactivity of gaseous nitric acid on authentic mineral dust samples, and on individual mineral and clay mineral components, Phys. Chem. Chem. Phys., 3, 2474-2482, 2001b.

Ho, K. F., Lee, S. C., Cao, J. J., Kawamura, K., Watanabe, T., Cheng, Y., and Chow, J. C.: Dicarboxylic acids, ketocarboxylic acids and dicarbonyls in the urban roadside area of Hong Kong, Atmos. Environ., 40, 3030-3040, 2006.

Huang, X. F., Yu, J. Z., He, L. Y., and Yuan, Z. B.: Water-soluble organic carbon and oxalate in aerosols at a coastal urban site in China: Size distribution characteristics, sources, and formation mechanisms, J. Geophys. Res., 111, D22212, doi:10.1029/2006JD007408, 2006.

Jacobson, M. Z.: Atmospheric Pollution: History, Science, and Regulation. Cambridge University Press, United Kingdom, 2002.

Jacobson, M. C., Hansson, H. C., Noone, K. J., and Charlson, R. J.: Organic atmospheric aerosols: Review and state of science, Rev. Geophys., 38, 267-294, 2000.

Jafferson, A., Tanner, D. J., Eisele, F. L., Davis, D. D., Chen, G., Creawford, J., Huey, J. W., Torres, A. L., and Berresheim, H.: OH photochemistry and methane sulfonic acid formation in the coastal Antarctic boundary layer, J. Geophys. Res., 103, 1647-1656, 1998.

Jung, J. S., Tsatsral, B., Kim, Y. J., and Kawamura, K.: Organic and inorganic aerosol compositions in Ulaanbaatar, Mongolia, during the cold winter of 2007 to 2008: Dicarboxylic acids, ketocarboxylic acids, and alpha-dicarbonyls, J. Geophys. Res., 115, D22203, doi:10.1029/2010JD014339, 2010.

Kampf, C. J., Corrigan, A. L., Johnson, A. M., Song, W., Keronen, P., Konigstedt, R., Williams, J., Russel, L. M., Petaja, T., Fischer, H., and Hoffmann, T.: First measurments of reactive alpha-dicarbonyl concentrations on $PM_{2.5}$ aerosols over the Boreal forest in Finland during HUMPPA-COPEC 2010 - source apportionment and links to aerosol aging, Atmos. Chem. Phys., 12, 6145-6155, 2012.

Kanakidou, M., Seinfeld, J. H., Pandis, S. N., Barnes, I., Dentener, F. J., Facchini, M. C., Van Dingenen, R., Ervens, B., Nenes, A., Nielsen, C. J., Swietlicki, E., Putaud, J. P., Balkanski, Y., Fuzzi, S., Horth, J., Moortgat, G. K., Winterhalter, R., Myhre, C. E. L., Tsigaridis, K., Vignati, E., Stephanou, E. G., and Wilson, J.: Organic aerosol and global climate modelling: a review, Atmos. Chem. Phys., 5, 1053-1123, 2005.

Kaufman, Y. J. and Fraser, R. S.: The effect of smoke particles on clouds and climate forcing, Science, 277, 1636-1639, 1997.

Kawamura, K. and Gagosian, R. B.: Implications of ω-oxocarboxylic acids in the remote marine atmosphere for photo-oxidation of unsaturated fatty acids, Nature, 325, 330-332, 1987.

Kawamura, K. and Ikushima, K.: Seasonal changes in the distribution of dicarboxylic acids in the urban atmosphere, Environ. Sci. Technol., 27, 2227-2235, 1993.

Kawamura, K. and Kaplan, I. R.: Motor Exhaust Emissions as a Primary Source for Dicarboxylic-Acids in Los-Angeles Ambient Air, Environ. Sci. Technol., 21, 105-110, 1987.

Kawamura, K. and Sakaguchi, F.: Molecular distributions of water soluble dicarboxylic acids in marine aerosols over the Pacific Ocean including tropics, J. Geophys. Res., 104, 3501-3509, 1999.

Kawamura, K. and Usukura, K.: Distributions of low molecular weight dicarboxylic acids in the North Pacific aerosol samples, J. Oceanogr., 49, 271-283, 1993.

870 Kawamura, K., Imai, Y., and Barrie, L. A.: Photochemical production and loss of organic acids in
871 high Arctic aerosols during long-range transport and polar sunrise ozone depletion events,
872 Atmos. Environ., 39, 599-614, 2005.

873 Kawamura, K., Kasukabe, H., and Barrie, L. A.: Source and reaction pathways of dicarboxylic
874 acids, ketoacids and dicarbonyls in arctic aerosols: One year of observations, Atmos.
875 Environ., 30, 1709-1722, 1996.

876 Kawamura, K., Narukawa, M., Li, S. M., and Barrie, L. A.: Size distributions of dicarboxylic acids
877 and inorganic ions in atmospheric aerosols collected during polar sunrise in the Canadian high
878 Arctic, J. Geophys. Res., 112, D10307, doi:10.1029/2006JD008244, 2007.

879 Kawamura, K., Ng, L., and Kaplan, I. R., Determination of organic acids (C_1-C_{10}) in the
880 atmosphere, motor-exhausts and engine oils, Environ. Sci. Technol., 19, 1082-1086, 1985.

881 Kawamura, K., Okuzawa, K., Aggarwal, S. G., Irie, H., Kanaya, Y., and Wang, Z.: Determination
882 of gaseous and particulate carbonyls (glycolaldehyde, hydroxyacetone, glyoxal,
883 methylglyoxal, nonanal and decanal) in the atmosphere at Mt. Tai, Atmos. Chem. Phys., 13,
884 5369-5380, 2013.

885 Kawamura, K. and Pavuluri, C.M.: New Directions: Need for better understanding of plastic waste
886 burning as inferred from high abundance of terephthalic acid in South Asian aerosols, Atmos.
887 Environ., 44, 5320-5321, 2011.

888 Kawamura, K., Steinberg, S., and Kaplan, I. R.: Homologous series of C_1-C_{10} monocarboxylic acids
889 and C_1-C_6 carbonyls in Los Angeles air and motor vehicle exhausts, Atmos. Environ., 34,
890 4175-4191, 2000.

891 Kawamura, K.: Identification of C_2-C_{10} ω-oxocarboxylic acids, pyruvic acid, and C_2-C_3 α-
892 dicarbonyls in wet precipitation and aerosol samples by capillary GC and GC/MS, Anal.
893 Chem., 65, 3505-3511, 1993.

894 Kerminen, V. -M., Pakkanen, T. A., and Hillamo, R. E.: Interactions between inorganic trace gases
895 and supermicrometer particles at a coastal site, Atmos. Environ., 31, 2753-2765, 1997a.

896 Kerminen, V. -M., Aurela, M., Hillamo, R. E., and Virkkula, A.: Formation of particualte MSA:
897 deductions from size distribution measurements in the Finnish Arctic, Tellus, 49b, 159-171,
898 1997b.

899 Kerminen, V. -M., Teinila, K., Hillamo, R., and Makela, T.: Size-segregated chemistry of
900 particulate dicarboxylic acids in the Arctic atmosphere, Atmos. Environ., 33, 2089-2100,
901 1999.

902 Kleeman, M. J. and Cass, G. R.: Effect of emissions control strategies on the size and composition
903 distribution of urban particulate air pollution, Environ. Sci. Technol., 33, 177-189, 1999.

904 Kouyoumdjian, H. and Saliba, N. A.: Mass concentration and ion composition of coarse and fine
905 particles in an urban area in Beirut: effect of calcium carbonate on the absorption of nitric and
906 sulfuric acids and the depletion of chloride, Atmos. Chem. Phys., 6, 1865-1877, 2006.

907 Kroll, J. H., Ng, N. L., Murphy, S. M., Varutbangkul, V., Flagan, R. C., and Seinfeld, J. H.:
908 Chamber studies of secondary organic aerosol growth by reactive uptake of simple carbonyl
909 compounds, J. Geophys. Res., 110, D23207, doi:10.1029/2005jd006004, 2005.

910 Kumar, A., Sarin, M. M., and Sudheer, A. K.: Mineral and anthropogenic aerosols in Arabian Sea-
911 atmospheric boundary layer: Sources and spatial variability, Atmos. Environ., 42, 5169-5181,
912 2008.

913 Kundu S., Kawamura, K., Andreae, T. W., Hoffer, A., and Andreae, M. O.: Molecular distributions
914 of dicarboxylic acids, ketocarboxylic acids and α-dicarbonyls in biomass burning aerosols:
915 implications for photochemical production and degradation in smoke layers, Atmos. Chem.
916 Phys., 10, 2209-2225, 2010.

917 Kunwar, B. and Kawamura, K.: Seasonal distribution and sources of low molecular weight
918 dicarboxylic acids, ω-oxocarboxylic acids, pyruvic acid, α-dicarbonyls and fatty acids in
919 ambient aerosols from subtropical Okinawa in the western Pacific Rim, Environ. Chem., 11,
920 673-689, 2014.

921 Legrand, M., Preunkert, S., Oliveira, T., Pio, C. A., Hammer, S., Gelencser, A., Kasper-Giebl, A.,
922 and Laj, P.: Origin of C_2-C_5 dicarboxylic acids in the European atmosphere inferred from
923 year-round aerosol study conducted at a west-east transect, J. Geophys. Res., 112, D23S07,
924 doi:10.1029/2006JD008019, 2007.

925 Liggio, J. L., Li, S. M., and McLaren, R.: Reactive uptake of glyoxal by particulate matter, J.
926 Geophys. Res., 110, D10304, doi:10.1029/2004JD005113, 2005.

927 Lim, H. J., Carlton, A. G., and Turpin, B. J.: Isoprene forms secondary organic aerosol through
928 cloud processing: Model simulations, Environ. Sci. Technol., 39, 4441-4446, 2005.

929 Lim, Y. B., Tan, Y., Perri, M. J., Seitzinger, S. P., and Turpin, B. J.: Aqueous chemistry and its role
930 in secondary organic aerosol (SOA) formation, Atmos. Chem. Phys., 10, 10521-10539, 2010.

931 Liu, S. Z., Tao, S., Liu, W. X., Liu, Y. N., Dou, H., Zhao, J. Y., Wang, L. G., Wang, J. F., Tian, Z.
932 F., and Gao, Y.: Atmospheric polycyclic aromatic hydrocarbons in north China: A winter-
933 time study, Environ. Sci. Technol., 41, 8256-8261, 2007.

934 Mayol-Bracero, O. L., Guyon, P., Graham, B., Roberts, G., Andreae, M. O., Decesari, S., Facchini,
935 M. C., Fuzzi, S., and Artaxo, P.: Water-soluble organic compounds in biomass burning
936 aerosols over Amazonia - 2. Apportionment of the chemical composition and importance of
937 the polyacidic fraction, J. Geophys. Res., 107, 8091, doi:10.1029/2001jd000522, 2002.

938 Meinardi, S., Simpson, I. J., Blake, N. J., Blake, D. R., and Rowland, E. S.: Dimethyl disulfide
939 (DMDS) and dimethyl sulfide (DMS) emissions from biomass burning in Australia, Geophys.
940 Res. Lett., 30, 1454, doi:10.1029/2003GL016967, 2003.

941 Mkoma, S. L., Kawamura, K., and Fu, P. Q.: Contributions of biomass/biofuel burning to organic
942 aerosols and particulate matter in Tanzania, East Africa, based on analyses of ionic species,
943 organic and elemental carbon, levoglucosan and mannosan, Atmos. Chem. Phys., 13, 10325-
944 10338, 2013.

945 Miyazaki, Y., Kawamura, K., and Sawano, M.: Size distributions and chemical characterization of
946 water-soluble organic aerosols over the western North Pacific in summer, J. Geophys. Res.,
947 115, D23210, doi:10.1029/2010JD014439, 2010.

948 Miyazaki, Y., Kawamura, K., Jung, J., Furutani, H., and Uematsu, M.: Latitudinal distributions of
949 organic nitrogen and organic carbon in marine aerosols over the western North Pacific,
950 Atmos. Chem. Phys., 11, 3037-3049, 2011.

951 Mochida, M., Kawamura, K., Umemoto, N., Kobayashi, M., Matsunaga, S., Lim, H. J., Turpin, B.
952 J., Bates, T. S., and Simoneit, B. R. T.: Spatial distributions of oxygenated organic
953 compounds (dicarboxylic acids, fatty acids, and levoglucosan) in marine aerosols over the
954 western Pacific and off the coast of East Asia: Continental outflow of organic aerosols during
955 the ACE-Asia campaign, J. Geophys. Res., 108, 8638, doi:10.1029/2002JD003249, 2003a.

956 Mochida, M., Umemoto, N., Kawamura, K., and Uematsu, M.: Bimodal size distribution of C_2-C_4
957 dicarboxylic acids in the marine aerosols, Geophys. Res. Lett., 30, 1672, doi:
958 10.1029/2003GL017451, 2003b.

959 Mochida, M., Umemoto, N., Kawamura, K., Lim, H. J., and Turpin, B. J.: Bimodal size
960 distributions of various organic acids and fatty acids in the marine atmosphere: Influence of
961 anthropogenic aerosols, Asian dusts, and sea spray off the coast of East Asia, J. Geophys.
962 Res., 112, D15209, doi:10.1029/2006JD007773, 2007.

963 Myriokefalitakis, S., Tsigaridis, K., Mihalopoulos, N., Sciare, J., Nenes, A., Kawamura, K., Segers,
964 A., and Kanakidou, M.: In-cloud oxalae formation in the regional troposphere: a 3-D
965 modelling study, Atmos. Chem. Phys., 11, 5761-5782, 2011.

966 Nenes, A., Pandis, S. N., and Pilinis, C.: ISORROPIA: A new thermodynamic equilibrium model
967 for multiphase multicomponent inorganic aerosols, Aquat. Geochem., 4, 123-152, 1998.

968 Pakkanen, T. A., Loukkola, K., Korhonen, C. H., Aurela, M., Makela, T., Hillamo, R. E., Aarnio,
969 P., Koskentalo, T., Kousa, A., and Maenhaut, W.: Sources and chemical composition of
970 atmospheric fine and coarse particles in the Helsinki area, Atmos. Environ., 35, 5381-5391,
971 2001.

972 Pavuluri, C. M., Kawamura, K., Mihalopoulos, N., and Swaminathan, T.: Laboratory
973 photochemical processing of aqueous aerosols: formaion and degradation of dicarboxylic
974 acids, oxocarboxylic acids, and alpha-dicarbonyls, Atmos. Chem. Phys., 15, 7999-8012, 2015.

975 Pope, C. A. and Dockery, D. W.: Health effects of fine particulate air pollution: Lines that connect,
976 J. Air Waste Manage., 56, 709-742, 2006.

977 Pradeep Kumar, P., Broekhuizen, K., and Abbatt, J. P. D.: Organic acids as cloud condensation
978 nuclei: Laboratory studies of highly soluble and insoluble species, Atmos. Chem. Phys., 3,
979 509-520, 2003.

980 Quinn, P. K., Covert, D. S., Bates, T. S., Kapustin, V. N., Ramseybell, D. C., and Mcinnes, L. M.:
981 Dimethylsulfide cloud condensation nuclei climate system - relevant size-resolved
982 measurements of the chemical and physical-properties of atmospheric aerosol-particles, J.
983 Geophys. Res., 98, 10411-10427, 1993.

984 Ramanathan, V., Crutzen, P. J., Kiehl, J. T., and Rosenfeld, D.: Atmosphere - Aerosols, climate,
985 and the hydrological cycle, Science, 294, 2119-2124, 2001.

986 Schauer, J. J., Rogge, W. F., Hildemann, L. M., Mazurek, M. A., and Cass, G. R.: Source
987 apportionment of airborne particualte matter using organic compounds as tracers, Atmos.
988 Environ., 30, 3837-3855, 1996.

989 Seinfeld, J. H. and Pandis, S. N.: Atmospheric chemistry and physics: From air pollution to climate
990 change, 2nd edition, J. Wiley, New York, 2006.

Seinfeld, J. H. and Pandis, S. N.: Atmospheric Chemistry and Physics, John Wiley & Sons, New York, 1998.

Seinfeld, J. H. and Pankow, J. F.: Organic atmospheric particulate material, Annu. Rev. Phys. Chem., 54, 121-140, 2003.

Sempéré, R. and Kawamura, K.: Trans-hemispheric contribution of C_2-C_{10} α,ω-dicarboxylic acids, and related polar compounds to water-soluble organic carbon in the western Pacific aerosols in relation to photochemical oxidation reactions, Glob. Biogeochem. Cycle, 17, 1069, doi:10.1029/2002GB001980, 2003.

Shimada, K., Shimida, M., Takami, A., Hasegawa, S., Akihiro, F., Arakaki, T., Izumi, W., and Hatakeyama, S.: Mode and place of origin of carbonaceous aerosols transported from East Asia to Cape Hedo, Okinawa, Japan, Aerosol Air. Qual. Res., 15, 799-813, 2015.

Simoneit, B. R. T., Medeiros, P. M., and Didyk, B. M.: Combustion products of plastics as indicators for refuse burning in the atmosphere, Environ. Sci. Technol., 39, 6961-6970, 2005.

Speer, R. E., Edney, E. O., and Kleindienst, T. E.: Impact of organic compounds on the concentrations of liquid water in ambient $PM_{2.5}$, J. Aerosol Sci., 34, 63-77, 2003.

Takami, A., Miyoshi, T., Shimono, A., Kaneyasu, N., Kato, S., Kajii, Y., and Hatakeyama, S.: Transport of anthropogenic aerosols from Asia and subsequent chemical transformation, J. Geophys. Res., 112, D22S31, doi 10.1029/2006jd008120, 2007.

Takiguchi, Y., Takami, A., Sadanaga, Y., Lun, X. X., Shimizu, A., Matsui, I., Sugimoto, N., Wang, W., Bandow, H., and Hatakeyama, S.: Transport and transformation of total reactive nitrogen over the East China Sea, J. Geophys. Res., 113, D10306, doi:10.1029/2007jd009462, 2008.

Tao, J., Zhang, L., Engling, G., Zhang, R., Yang, T., Cao, J., Zhu, C., Wang, Q., and Luo, L.: Chemical composition of $PM_{2.5}$ in an urban environment in Chengdu, China: Importance of springtime dust storms and biomass burning, Atmos. Res., 122, 270-283, 2013.

Tao, S., Wang, Y., Wu, S. M., Liu, S. Z., Dou, H., Liu, Y. N., Lang, C., Hu, F., and Xing, B. S.: Vertical distribution of polycyclic aromatic hydrocarbons in atmospheric boundary layer of Beijing in winter, Atmos. Environ., 41, 9594-9602, 2007.

Tsai, Y. I. and Chen, C. L.: Characterization of Asian dust storm and non-Asian dust storm $PM_{2.5}$ aerosol in southern Taiwan, Atmos. Environ., 40, 4734-4750, 2006.

Turpin, B. J. and Lim, H. J.: Species contributions to $PM_{2.5}$ mass concentrations: Revisiting common assumptions for estimating organic mass, Aerosol. Sci. Tech., 35, 602-610, 2001.

Volkamer, R., Platt, U., and Wirtz, K.: Primary and secondary glyoxal formation from aromatics: Experimental evidence for the bicycloalkyl-radical pathway from benzene, toluene, and p-xylene, J. Phys. Chem. A, 105, 7865-7874, 2001.

Wang, G. H., Kawamura, K., Xie, M. J., Hu, S. Y., Li, J. J., Zhou, B. H., Cao, J. J., and An, Z. S.: Selected water-soluble organic compounds found in size-resolved aerosols collected from urban, mountain and marine atmospheres over East Asia, Tellus, 63, 371-381, 2011.

Wang, G. H., Zhao, B. H., Cheng, C. L., Cao, J. J., Li, J. J., Meng, J. J., Tao, J., Zhang, R. J., and Fu, P. Q.: Impact of Gobi desert dust on aerosol chemistry of Xi'an, inland China during

1030 spring 2009: differences in composition and size distribution between the urban ground
1031 surface and the mountain atmosphere, Atmos. Chem. Phys., 13, 819-835, 2013.

1032 Wang, H., Kawamura, K., and Shooter, D.: Carbonaceous and ionic components in wintertime
1033 atmospheic aeosols from two New Zwaland cities: Implication for solid fuel combustion,
1034 Atmos. Environ., 39, 5865-5875, 2005a.

1035 Wang, Y., Zhuang, G. S., Sun, Y., and An, Z. S.: Water-soluble part of the aerosol in the dust storm
1036 season - evidence of the mixing between mineral and pollution aerosols, Atmos. Environ., 39,
1037 7020-7029, 2005b.

1038 Warneck, P.: In-cloud chemistry opens pathway to the formation of oxalic acid in the marine
1039 atmosphere, Atmos. Environ., 37, 2423-2427, 2003.

1040 Yamasoe, M. A., Artaxo, P., Miguel, A. H., and Allen, A. G.: Chemical composition of aerosol
1041 particles from direct emissions of vegetation fires in the Amazon Basin: water-soluble species
1042 and trace elements, Atmos. Environ., 34, 1641-1653, 2000.

1043 Zimmermann, J. and Poppe, D.: A supplement for the RADM2 chemical mechanism: The
1044 photooxidation of isoprene, Atmos. Environ., 30, 1255-1269, 1996.

Table 1. Concentrations (μg m^{-3}) of carbonaceous species and major inorganic ions in the fine and coarse mode aerosols in Okinawa Island in the Western North Pacific.

Inorganic ions	Fine mode[a]				Coarse mode[b]			
	Mean	S.D.[c]	Min.[d]	Max.[e]	Mean	S.D.	Min.	Max.
	Water-soluble inorganic ions							
	Cations							
Na^+	0.44	0.20	0.21	0.72	2.42	0.89	1.60	3.65
NH_4^+	2.40	1.18	0.74	3.69	0.03	0.01	0.03	0.05
K^+	0.14	0.06	0.04	0.21	0.09	0.02	0.07	0.12
Mg^{2+}	0.07	0.02	0.04	0.10	0.34	0.11	0.24	0.49
Ca^{2+}	0.06	0.02	0.04	0.09	0.41	0.19	0.15	0.60
Total cations	3.12	1.22	1.28	4.37	3.29	1.02	2.55	4.82
	Anions							
MSA^-	0.04	0.01	0.03	0.06	0.01	0.00	0.00	0.01
Cl^-	0.12	0.13	0.02	0.29	4.27	2.25	1.77	7.25
NO_3^-	0.14	0.08	0.04	0.23	1.61	0.54	0.94	2.41
SO_4^{2-}	10.1	4.85	2.88	14.9	1.46	0.44	0.69	1.81
Total anions	10.4	4.73	3.33	15.1	7.35	2.20	5.69	10.6
	Total water-soluble ions							
Total water-soluble ions	13.5	5.95	4.61	19.5	10.6	3.22	8.33	15.4
	Carbonaceous components							
WSOC	1.12	0.49	0.31	1.61	0.33	0.13	0.15	0.52
OC	1.62	0.59	0.62	2.12	0.60	0.17	0.36	0.82
OM	3.43	1.31	1.30	4.87	1.25	0.36	0.75	1.73
EC	0.05	0.03	0.00	0.09	-	-	-	-
TC	1.67	0.65	0.62	2.41	0.60	0.17	0.36	0.82

[a]Fine mode represents aerosol size of $D_p < 2.1$ μm.
[b]Coarse mode represents aerosol size of $D_p > 2.1$ μm.
[c]Standard deviation.
[d]Minimum.
[e]Maximum.

Table 2. Concentrations (ng m^{-3}) of water-soluble dicarboxylic acids and related polar compounds in the fine and coarse mode aerosols in Okinawa Island in the Western North Pacific.

Compounds	Abbreviation	Chemical formula	Fine mode[a]				Coarse mode[b]			
			Mean	S.D.[c]	Min.[d]	Max.[e]	Mean	S.D.	Min.	Max.
			Dicarboxylic acids							
Saturated normal-chain diacids										
Oxalic	C_2	HOOC-COOH	135	37.4	76.0	176	40.2	14.7	22.1	60.0
Malonic	C_3	HOOC-CH_2-COOH	19.5	6.84	7.56	23.6	12.4	3.52	6.87	15.5
Succinic	C_4	HOOC-$(CH_2)_2$-COOH	13.4	4.98	5.08	17.5	8.02	2.21	4.66	10.1
Glutaric	C_5	HOOC-$(CH_2)_3$-COOH	3.30	1.54	1.00	4.75	1.89	0.57	1.07	2.66
Adipic	C_6	HOOC-$(CH_2)_4$-COOH	3.49	1.09	2.47	4.98	2.50	1.24	1.45	4.23
Pimelic	C_7	HOOC-$(CH_2)_5$-COOH	0.46	0.24	0.04	0.63	0.32	0.11	0.20	0.44
Suberic	C_8	HOOC-$(CH_2)_6$-COOH	0.07	0.07	0.00	0.16	0.04	0.02	0.02	0.07
Azelaic	C_9	HOOC-$(CH_2)_7$-COOH	1.20	0.72	0.51	2.41	1.15	0.60	0.49	2.10
Decanedioic	C_{10}	HOOC-$(CH_2)_8$-COOH	0.17	0.11	0.01	0.30	0.08	0.07	0.03	0.19
Undecanedioic	C_{11}	HOOC-$(CH_2)_9$-COOH	0.47	0.33	0.13	0.76	0.25	0.10	0.14	0.38
Dodecanedioic	C_{12}	HOOC-$(CH_2)_{10}$-COOH	0.07	0.03	0.03	0.09	0.05	0.02	0.02	0.07
Branched-chain diacids										
Methylmalonic	iC_4	HOOC-CH(CH_3)-COOH	0.43	0.23	0.09	0.71	0.47	0.37	0.09	0.99
Methylsuccinic	iC_5	HOOC-CH(CH_3)-COOH	0.81	0.27	0.37	1.00	0.59	0.13	0.45	0.80
2-Methylglutaric	iC_6	HOOC-CH(CH_3)-$(CH_2)_2$-COOH	0.35	0.24	0.05	0.70	0.19	0.20	0.04	0.53
Unsaturated aliphatic diacids										
Maleic	M	HOOC-CH=CH-COOH - *cis*	0.81	0.25	0.41	1.05	0.73	0.23	0.37	0.95
Fumaric	F	HOOC-CH=CH-COOH - *trans*	0.31	0.09	0.20	0.42	0.21	0.08	0.12	0.30
Methylmaleic	mM	HOOC-C(CH_3)=CH-COOH - *cis*	0.34	0.27	0.11	0.76	0.57	0.48	0.11	1.37
Unsaturated aromatic diacids										
Phthalic	Ph	HOOC-(C_6H_4)-COOH - *o-isomer*	6.29	2.85	1.99	9.3	2.79	0.81	1.85	3.9
Isophthalic	iPh	HOOC-(C_6H_4)-COOH - *m-isomer*	0.46	0.07	0.35	0.55	0.17	0.06	0.09	0.22
Terephthalic	tPh	HOOC-(C_6H_4)-COOH - *p-isomer*	2.21	1.15	0.32	3.30	0.64	0.38	0.09	1.17
Multifunctional diacids										
Malic	hC_4	HOOC-CH(OH)-CH_2-COOH	0.14	0.05	0.11	0.21	0.14	0.06	0.07	0.20
Ketomalonic	kC_3	HOOC-C(O)-COOH	4.92	3.79	0.46	9.28	0.49	0.17	0.32	0.77
4-Ketopimelic	kC_7	HOOC-CH_2-CH_2-HC(O)$(CH_2)_2$-COOH	2.57	0.83	1.26	3.20	0.43	0.16	0.26	0.69
Total diacids			196	58.1	98.3	253	74.1	24.3	41.4	105
			ω-Oxocarboxylic acids							
Glyoxylic	ωC_2	OHC-COOH	14.1	5.92	4.77	20.2	4.81	2.00	2.23	7.20
3-Oxopropanoic	ωC_3	OHC-CH_2-COOH	0.08	0.05	0.00	0.12	0.05	0.04	0.02	0.12
4-Oxobutanoic	ωC_4	OHC-$(CH_2)_2$-COOH	2.23	1.12	0.86	3.56	0.68	0.35	0.41	1.22
9-Oxononanoic	ωC_9	OHC-$(CH_2)_7$-COOH	0.74	0.20	0.54	1.07	1.06	0.34	0.57	1.41
Total oxoacids			17.1	7.04	6.27	25.0	6.60	2.33	3.26	9.52
			Ketoacid							
Pyruvic	Pyr	CH_3-C(O)-COOH	2.61	0.76	1.67	3.48	2.32	1.20	0.76	4.09
			α-Dicarbonyls							
Glyoxal	Gly	OHC-CHO	2.74	1.12	1.45	4.40	0.84	0.26	0.50	1.17
Methylglyoxal	MeGly	CH_3-C(O)-CHO	1.09	0.98	0.25	2.53	0.65	0.16	0.45	0.87
Total α-dicarbonyls			2.83	1.59	1.03	4.68	1.49	0.37	0.96	1.86
			Aromatic monoacid							
Benzoic acid		H_5C_6-COOH	16.5	11.0	4.57	28.3	1.98	1.01	0.70	3.38

[a]Fine mode represents aerosol size of $D_p < 2.1$ μm.
[b]Coarse mode represents aerosol size of $D_p > 2.1$ μm.
[c]Standard deviation.
[d]Minimum.
[e]Maximum.

Table 3. Pearson correlation coefficients[a] (r) matrix among the selected measured chemical species/components in the fine and coarse mode aerosols in Okinawa Island in the Western North Pacific Rim.

	Fine mode[b]																				
	Na^+	NH_4^+	K^+	Mg^{2+}	Ca^{2+}	MSA^-	Cl^-	NO_3^-	SO_4^{2-}	WSOC	OC	C_2	C_3	C_4	C_5	C_9	Ph	ωC_2	Pyr	Gly	MeGly	LWC
Na^+	1.00																					
NH_4^+	-0.25	1.00																				
K^+	-0.32	0.99	1.00																			
Mg^{2+}	0.98	-0.16	-0.23	1.00																		
Ca^{2+}	-0.21	0.62	0.33	-0.15	1.00																	
MSA^-	-0.32	0.92	0.92	-0.17	0.53	1.00																
Cl^-	0.65	-0.85	-0.85	0.58	-0.33	-0.78	1.00															
NO_3^-	0.65	-0.56	-0.55	0.68	0.22	-0.36	0.76	1.00														
SO_4^{2-}	-0.10	0.99	0.98	-0.02	0.59	0.89	-0.78	-0.49	1.00													
WSOC	0.10	0.91	0.93	0.16	0.30	0.79	-0.57	-0.27	0.96	1.00												
OC	0.12	0.91	0.95	0.16	0.25	0.80	-0.57	-0.32	0.93	0.99	1.00											
C_2	0.12	0.89	0.85	-0.13	0.22	0.80	-0.53	-0.30	0.92	0.99	0.98	1.00										
C_3	-0.05	0.90	0.89	-0.05	0.20	0.66	-0.68	-0.53	0.90	0.93	0.96	0.89	1.00									
C_4	-0.12	0.96	0.95	-0.09	0.15	0.76	-0.75	-0.55	0.96	0.95	0.96	0.92	0.99	1.00								
C_5	-0.12	0.99	0.96	-0.05	0.33	0.87	-0.80	-0.53	0.99	0.93	0.93	0.91	0.95	0.97	1.00							
C_9	0.64	0.01	0.02	0.61	0.42	-0.16	0.46	0.47	0.10	0.20	0.39	0.38	0.33	0.23	0.09	1.00						
Ph	0.41	0.78	0.73	0.46	0.42	0.63	-0.40	-0.16	0.87	0.92	0.93	0.90	0.83	0.83	0.86	0.23	1.00					
ωC_2	0.11	0.92	0.90	0.19	0.19	0.82	-0.57	-0.25	0.96	0.99	0.99	0.99	0.90	0.93	0.95	0.36	0.93	1.00				
Pyr	0.01	0.93	0.88	0.12	0.39	0.88	-0.73	-0.33	0.96	0.88	0.87	0.85	0.80	0.86	0.96	0.03	0.38	0.91	1.00			
Gly	0.01	0.86	0.86	0.15	0.09	0.92	-0.52	-0.07	0.86	0.89	0.82	0.93	0.70	0.78	0.85	0.21	0.85	0.92	0.85	1.00		
MeGly	0.15	0.35	0.39	0.26	0.13	0.52	0.06	0.50	0.36	0.53	0.35	0.62	0.25	0.31	0.31	0.48	0.36	0.55	0.29	0.75	1.00	
LWC	0.16	0.87	0.83	0.30	0.53	0.88	-0.53	-0.13	0.92	0.90	0.87	0.92	0.82	0.83	0.89	0.18	0.90	0.95	0.95	0.95	0.55	1.00
	Coarse mode[c]																					
	Na^+	NH_4^+	K^+	Mg^{2+}	Ca^{2+}	MSA^-	Cl^-	NO_3^-	SO_4^{2-}	WSOC	OC	C_2	C_3	C_4	C_5	C_9	Ph	ωC_2	Pyr	Gly	MeGly	LWC
Na^+	1.00																					
NH_4^+	0.60	1.00																				
K^+	0.96	0.77	1.00																			
Mg^{2+}	0.98	0.63	0.33	1.00																		
Ca^{2+}	-0.12	0.03	-0.06	-0.29	1.00																	
MSA^-	-0.15	-0.66	-0.03	-0.25	-0.02	1.00																
Cl^-	0.98	0.59	0.90	0.98	-0.27	-0.22	1.00															
NO_3^-	-0.30	-0.23	-0.15	-0.39	0.98	0.28	-0.55	1.00														
SO_4^{2-}	0.33	0.32	0.56	0.28	0.63	0.25	0.16	0.67	1.00													
WSOC	-0.18	-0.26	0.06	-0.20	0.23	0.55	-0.36	0.92	0.72	1.00												
OC	-0.11	-0.10	0.13	-0.10	0.21	0.36	-0.28	0.92	0.72	0.97	1.00											
C_2	-0.05	0.26	0.30	0.15	0.63	0.09	-0.08	0.88	0.76	0.93	0.82	1.00										
C_3	0.32	0.33	0.53	0.31	0.68	0.18	0.15	0.75	0.92	0.88	0.82	0.93	1.00									
C_4	0.33	0.39	0.60	0.35	0.53	0.16	0.33	0.32	0.88	0.31	0.55	0.36	0.63	1.00								
C_5	0.05	0.05	0.22	-0.06	0.62	0.32	-0.05	0.43	0.75	0.28	0.38	0.22	0.45	0.91	1.00							
C_9	0.85	0.20	0.25	0.91	-0.16	-0.59	0.85	-0.31	0.18	-0.08	-0.25	0.25	0.30	0.19	-0.23	1.00						
Ph	-0.52	-0.54	-0.29	-0.54	0.73	0.59	-0.66	0.93	0.54	0.56	0.33	0.63	0.58	0.21	0.40	-0.58	1.00					
ωC_2	0.23	0.37	0.85	0.68	0.12	0.42	0.59	0.23	0.73	0.53	0.52	0.53	0.76	0.60	0.32	0.23	0.21	1.00				
Pyr	-0.09	-0.01	0.13	-0.08	0.81	0.23	-0.26	0.93	0.73	0.99	0.93	0.96	0.90	0.33	0.28	-0.01	0.22	0.49	1.00			
Gly	0.26	0.26	0.78	0.57	0.05	0.52	0.58	0.06	0.69	0.28	0.33	0.22	0.55	0.76	0.57	0.24	0.12	0.89	0.21	1.00		
MeGly	0.55	0.69	0.67	0.58	0.48	-0.20	0.48	0.18	0.77	0.16	0.13	0.25	0.58	0.93	0.75	0.46	-0.05	0.49	0.22	0.59	1.00	
LWC	0.61	0.03	0.53	0.56	-0.70	0.48	0.63	-0.51	-0.10	-0.19	-0.13	-0.29	-0.08	-0.03	-0.22	0.23	-0.31	0.57	-0.28	0.63	-0.13	1.00

See Table 1 and 2 for abbreviation.

[a]Correlation is significant at 0.05 level for the values where r is > 0.80.

[b]Fine mode represents aerosol size of $D_p < 2.1$ μm.

[c]Coarse mode represents aerosol size of $D_p > 2.1$ μm.

1045 **Figure Captions**

1046 **Figure 1.** A map of East Asia with the location of Okinawa Island (26.87°N and 128.25°E) and
1047 major megacities in Asia.

1048 **Figure 2.** NOAA HYSPLIT seven-day backward air mass trajectories at 500 m a.g.l. for the aerosol
1049 samples (OKI-1 to OKI-5) at Okinawa Island. The dates given in each panel in figure are the
1050 starting and ending date of collection of aerosol samples in Okinawa Island.

1051 **Figure 3.** Average size-segregated chemical composition of spring aerosols collected at Okinawa
1052 Island.

1053 **Figure 4.** Average molecular distributions of water-soluble dicarboxylic acids and related
1054 compounds in size-segregated aerosols collected at Okinawa Island.

1055 **Figure 5.** Size distributions of water-soluble inorganic ions in the aerosol samples collected at
1056 Okinawa Island.

1057 **Figure 6.** Aerosol liquid water contents for each sample in size-segregated aerosols and mean liquid
1058 water contents of size-segregated aerosols at Okinawa Island.

1059 **Figure 7.** Size distributions of selected water-soluble dicarboxylic acids and related compounds in
1060 the aerosol samples collected at Okinawa Island.

1061 **Figure 8.** Size distributions of water-soluble organic carbon (WSOC) and organic carbon (OC) in
1062 the aerosol samples collected at Okinawa Island.

1063 **Figure 9.** Mass concentration ratio of malonic to succinic acid and phthalic to azelaic acid in size-
1064 segregated aerosols collected at Okinawa Island.

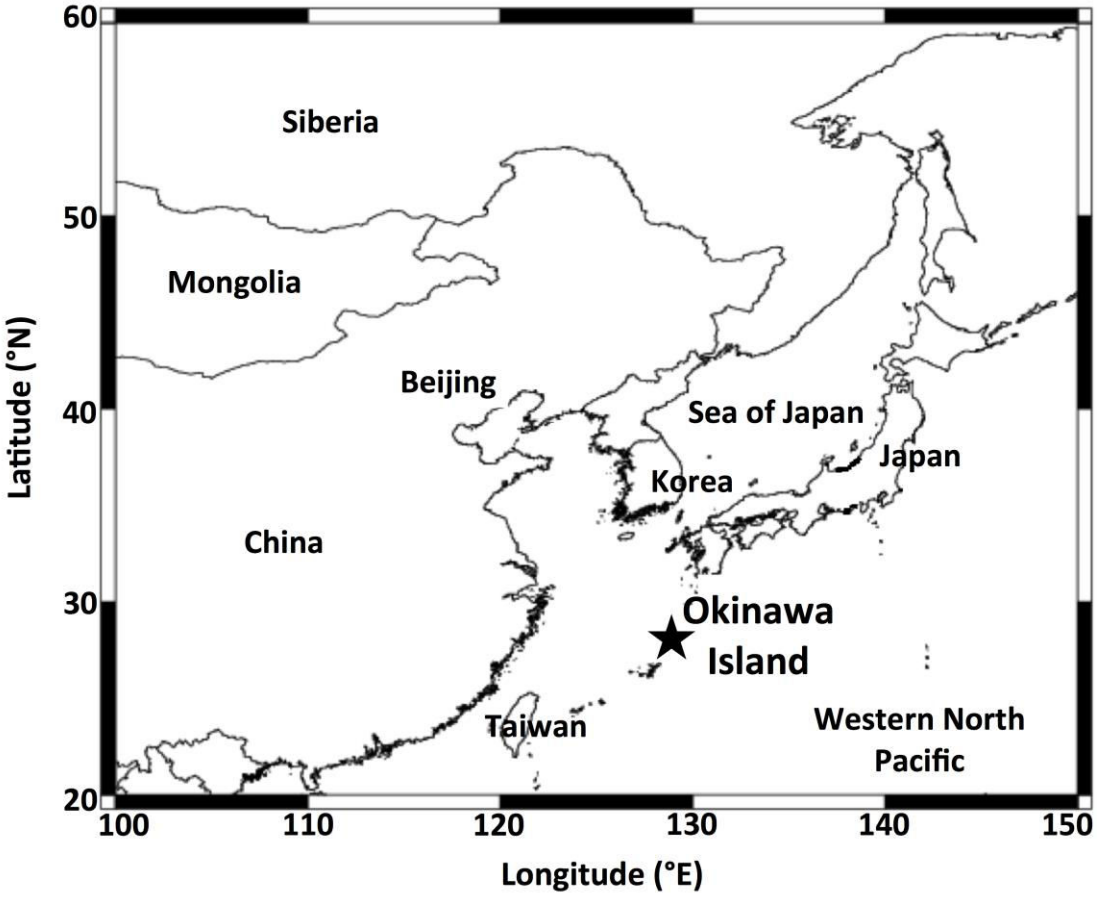

1065

1066 **Figure 1.** A map of East Asia with the location of Okinawa Island (26.87°N and 128.25°E) and

1067 major megacities.

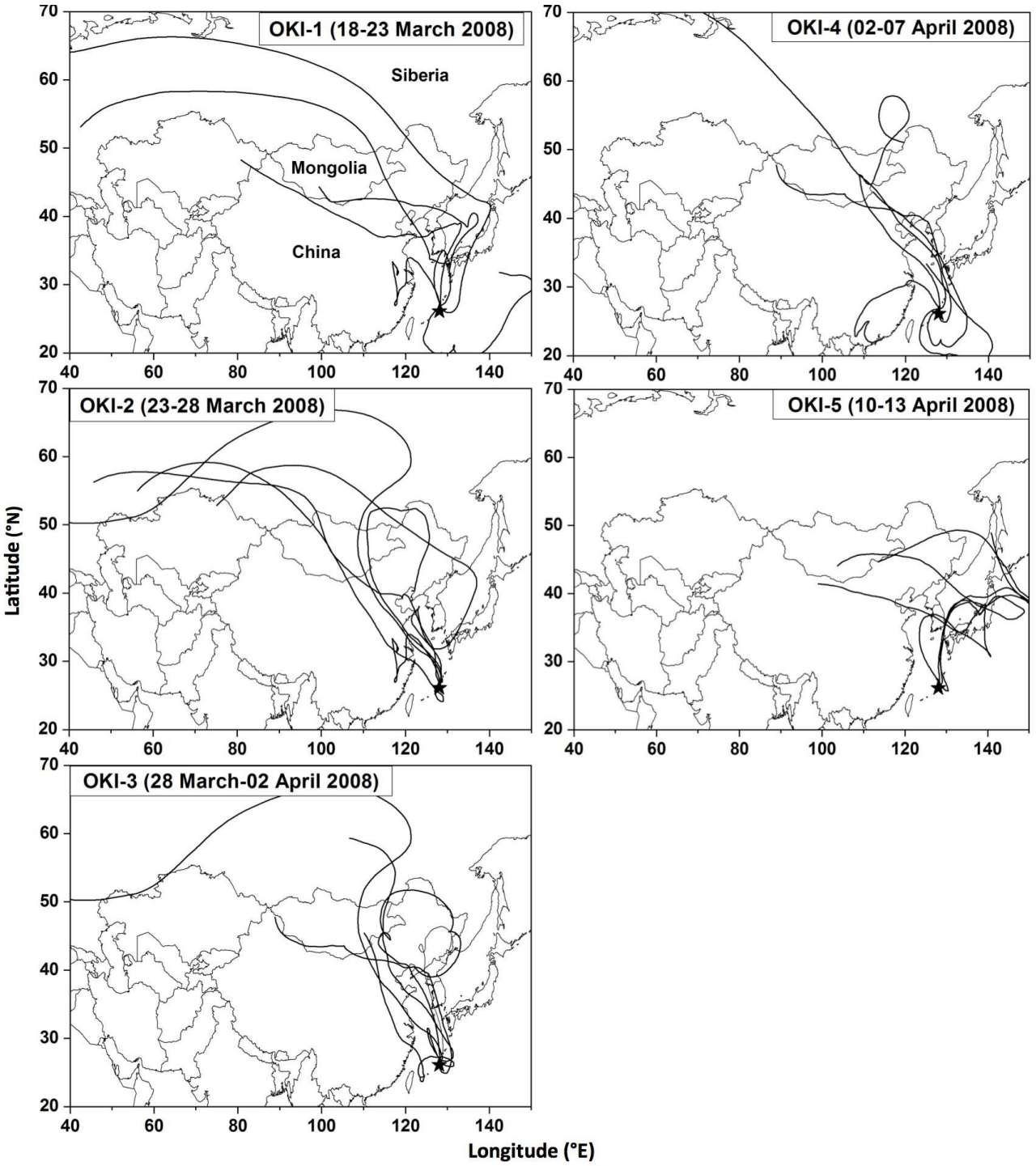

Figure 2. NOAA HYSPLIT seven-day backward air mass trajectories at 500 m a.g.l. for the aerosol samples (OKI-1 to OKI-5) at Okinawa Island. The dates given in each panel in figure are the starting and ending date of collection of aerosol samples in Okinawa Island.

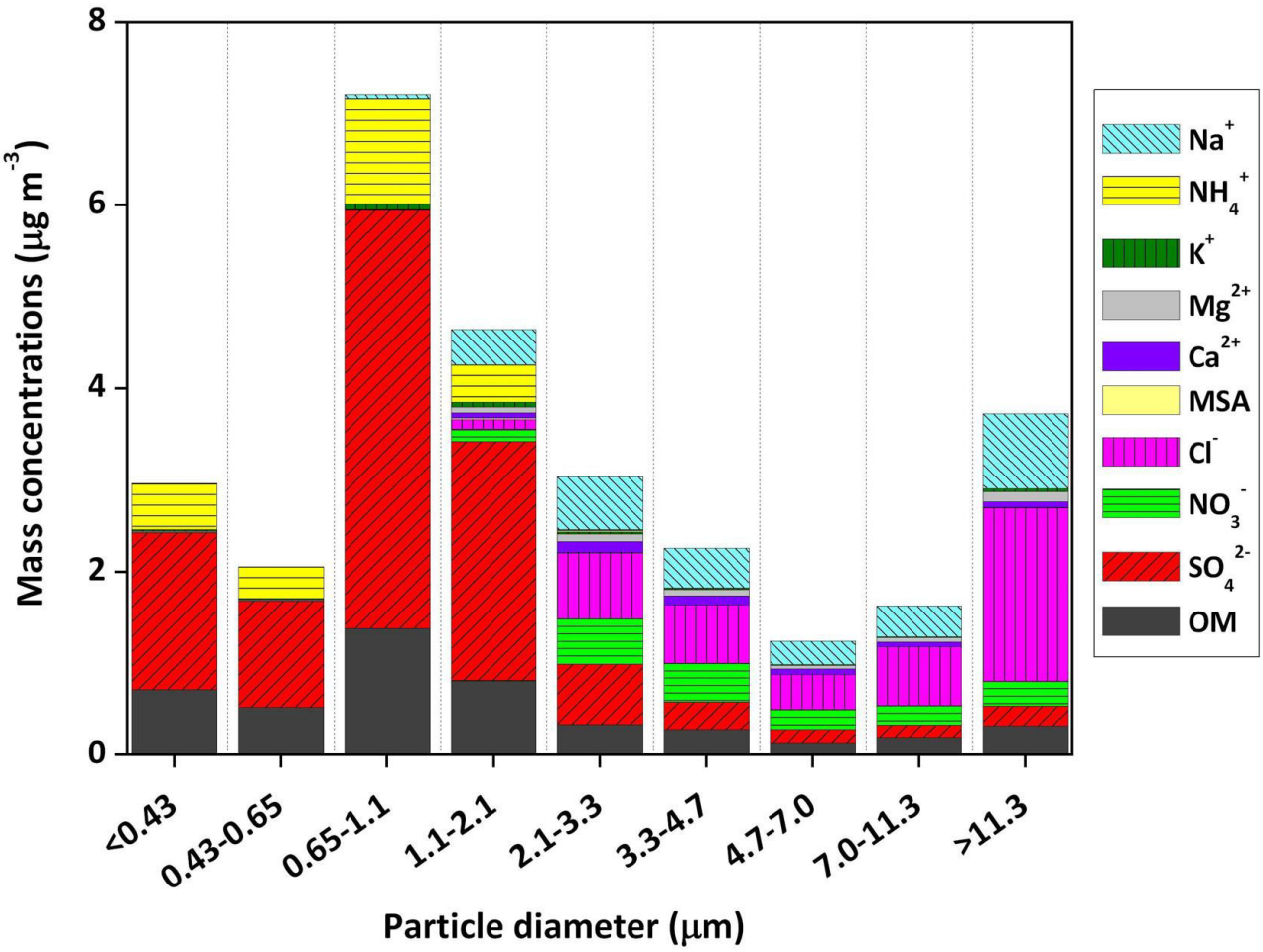

1072

1073 **Figure 3.** Average size-segregated chemical composition of spring aerosols collected at Okinawa

1074 Island.

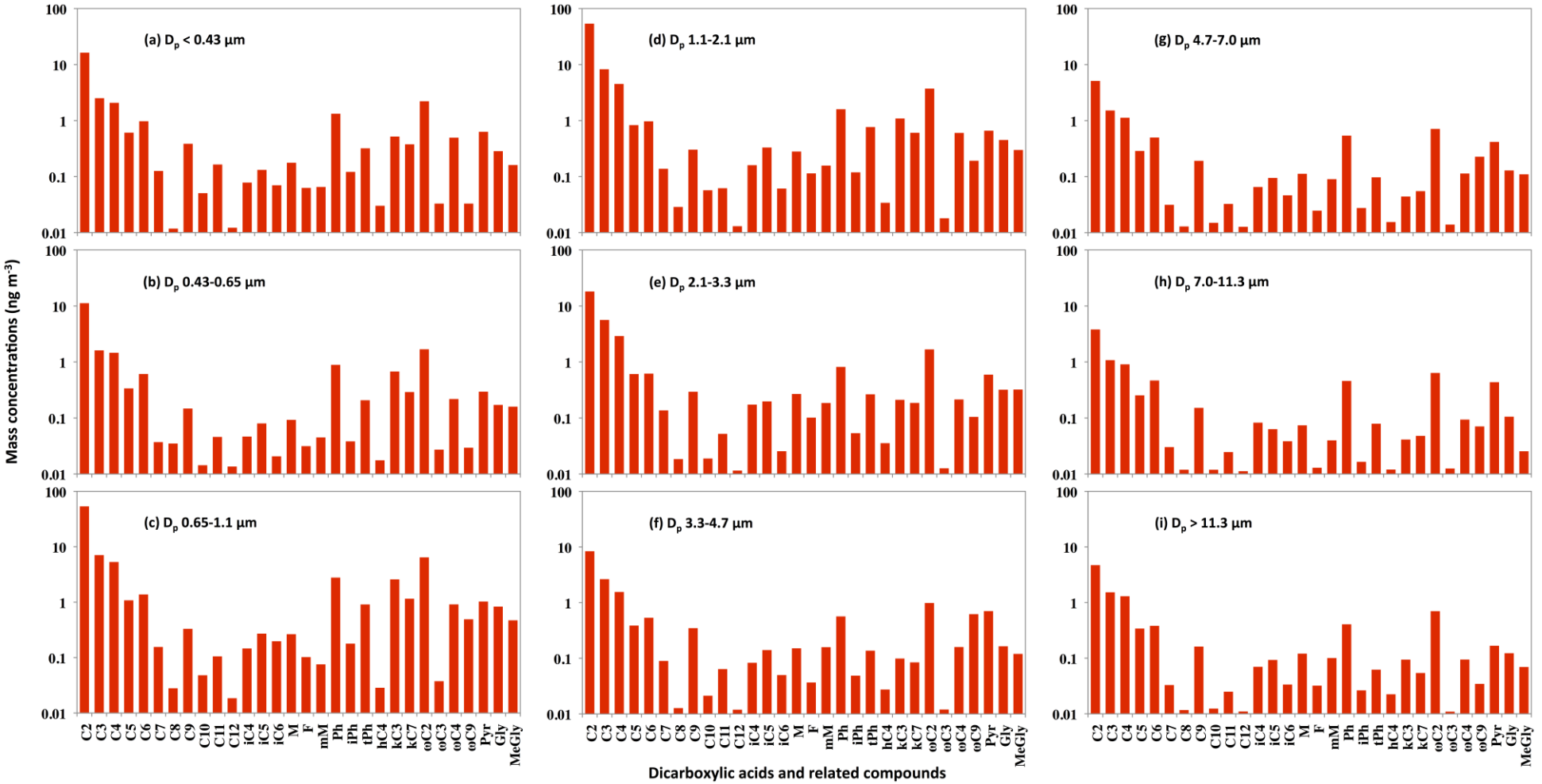

Figure 4. Average molecular distributions of water-soluble dicarboxylic acids and related compounds in size-segregated aerosols collected at Okinawa Island.

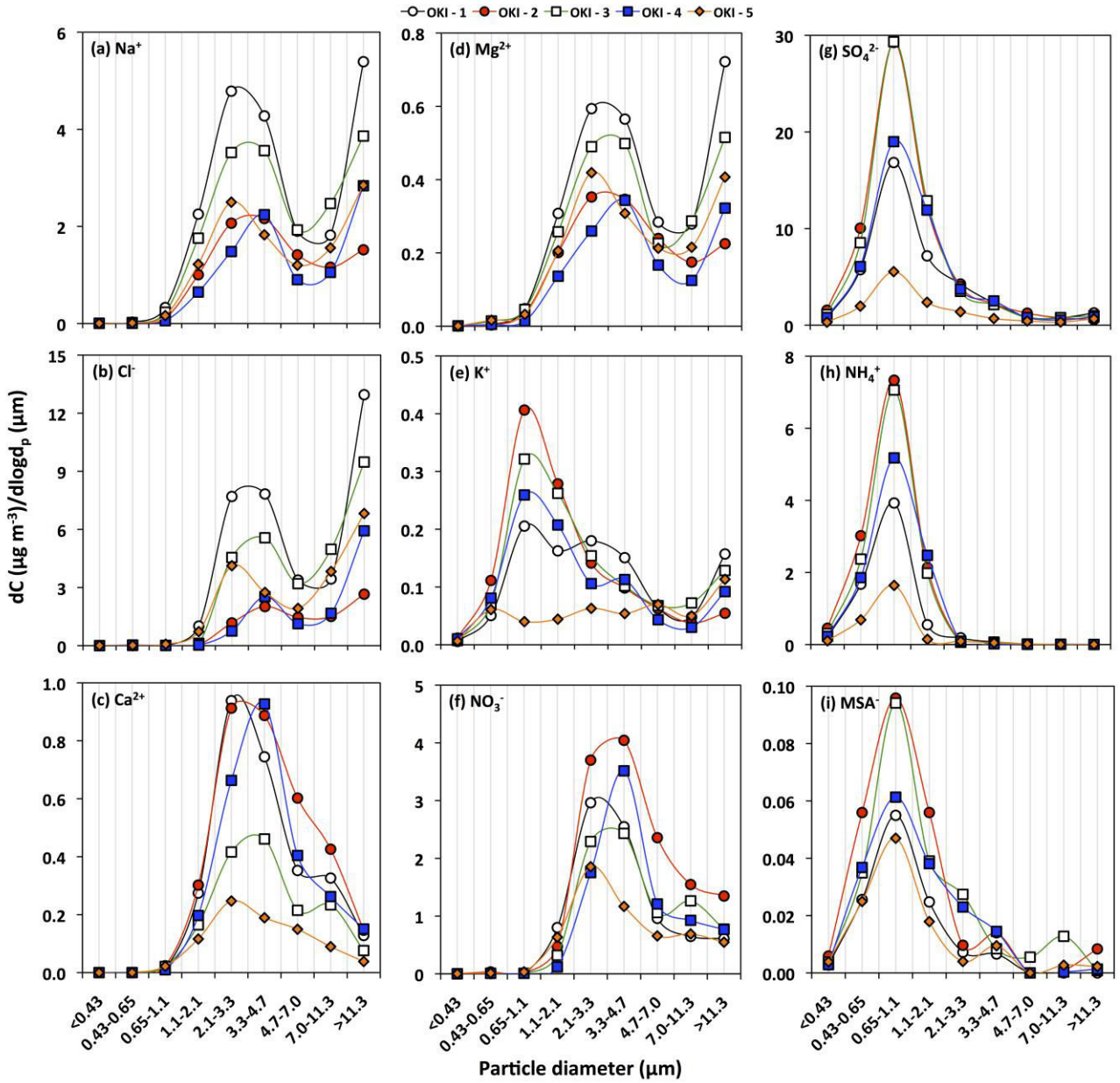

1078

1079 **Figure 5.** Size distributions of water-soluble inorganic ions in the aerosol samples collected at

1080 Okinawa Island.

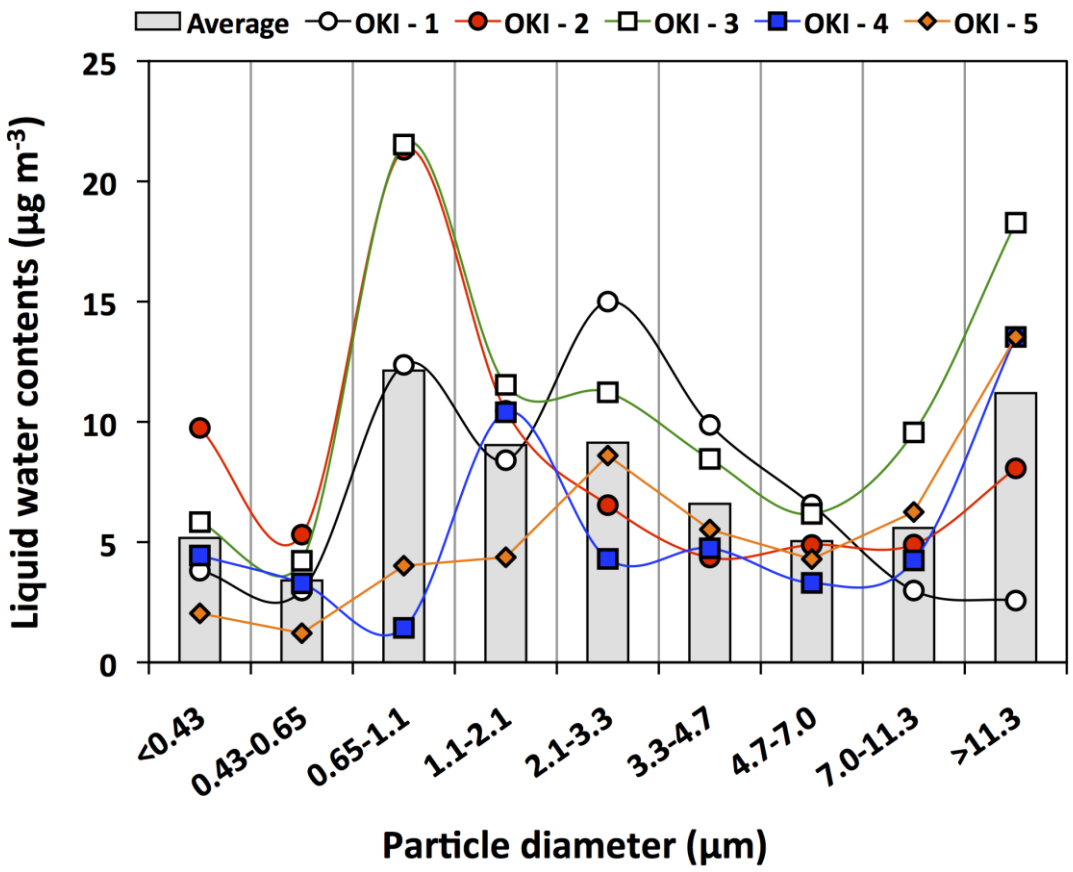

1081

1082 **Figure 6.** Aerosol liquid water contents for each sample in size-segregated aerosols and mean liquid

1083 water contents of size-segregated aerosols at Okinawa Island.

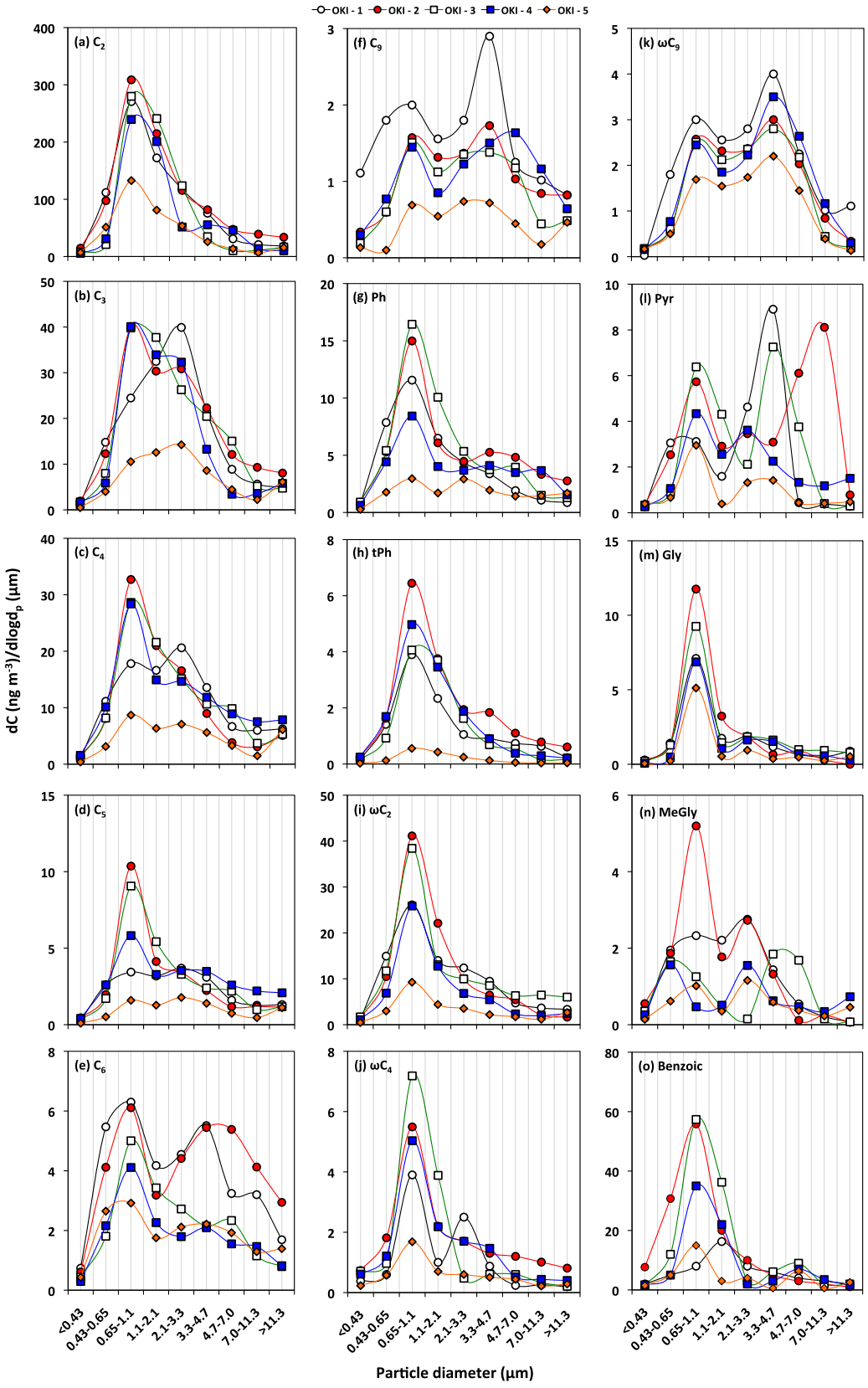

Figure 7. Size distributions of selected water-soluble dicarboxylic acids and related compounds in the aerosol samples collected at Okinawa Island.

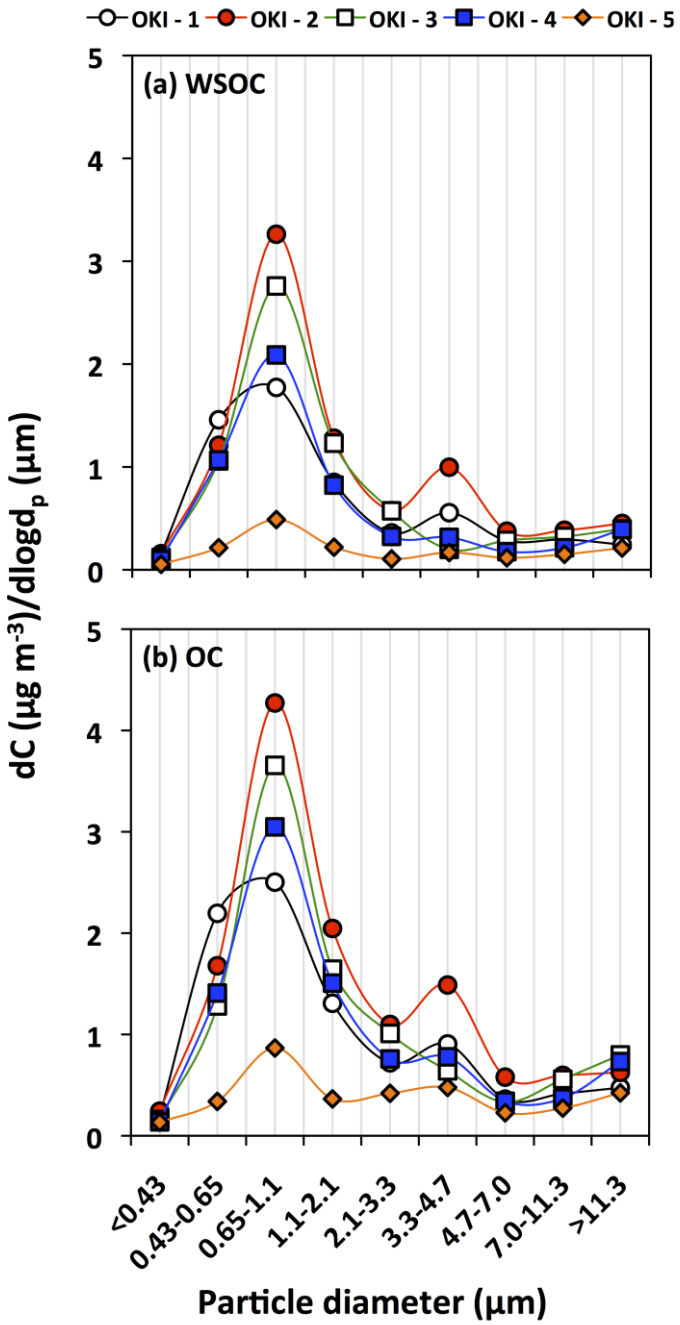

Figure 8. Size distributions of water-soluble organic carbon (WSOC) and organic carbon (OC) in the aerosol samples collected at Okinawa Island.

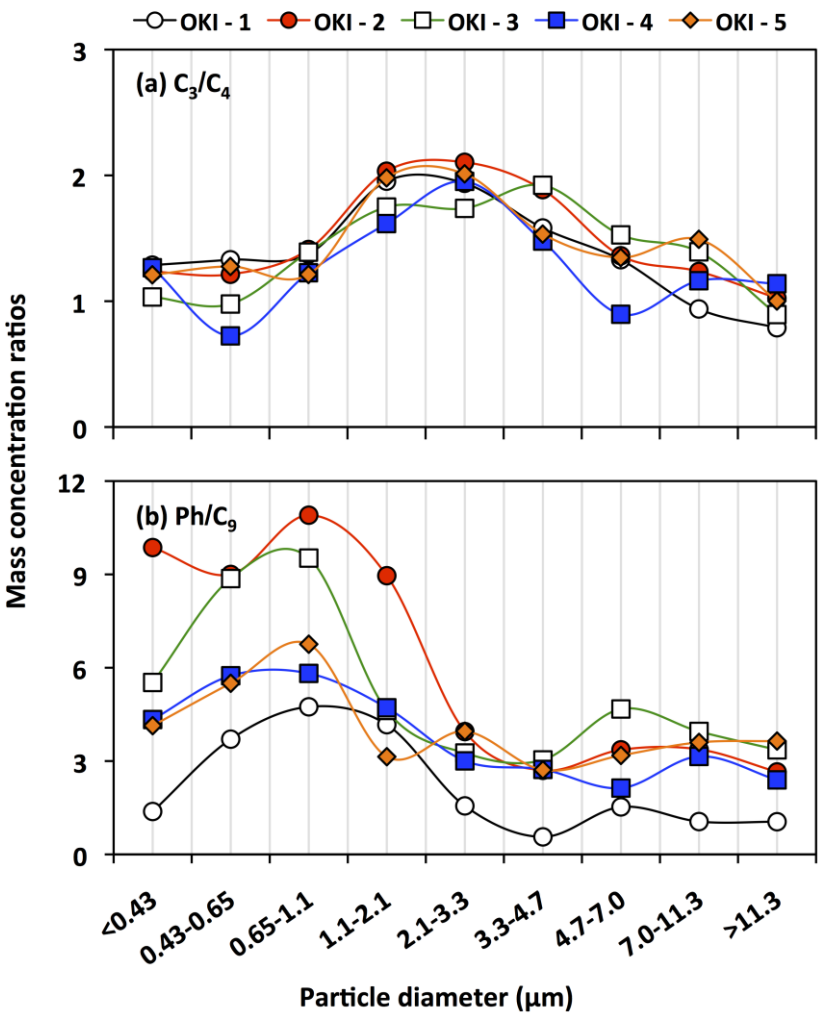

1091

1092 **Figure 9.** Mass concentration ratio of malonic to succinic acid and phthalic to azelaic acid in size-

1093 segregated aerosols collected at Okinawa Island.